# Integration of the *Salmonella* Typhimurium methylome and transcriptome reveals DNA methylation and transcriptional regulation are largely decoupled under virulence-related conditions

Jeffrey S. Bourgeois[a,b], Caroline E. Anderson[a], Liuyang Wang[a], Jennifer L. Modliszewski[c], Wei Chen[c], Benjamin H. Schott[a,b], Nicolas Devos[c], Dennis C. Ko[a,b,d]

**Affiliations**

[a] Department of Molecular Genetics and Microbiology, School of Medicine, Duke University, Durham, NC, 27710, USA
[b] University Program in Genetics and Genomics, Duke University, Durham, NC, 27710, USA
[c] Center for Genomics and Computational Biology, Duke University, Durham, NC, 27710, USA.
[d] Division of Infectious Diseases, Department of Medicine, School of Medicine, Duke University, Durham, NC, 27710, USA

*To whom correspondence should be addressed: Dennis C. Ko, 0048B CARL Building Box 3053, 213 Research Drive, Durham, NC 27710. 919-684-5834. dennis.ko@duke.edu.

@denniskoHiHOST

## Abstract

Despite being in a golden age of bacterial epigenomics, little work has systematically examined the plasticity and functional impacts of the bacterial DNA methylome. Here, we leveraged SMRT sequencing to examine the $m^6A$ DNA methylome of two *Salmonella enterica* ser. Typhimurium strains: 14028s and a Δ*metJ* mutant with derepressed methionine metabolism, grown in Luria Broth or a media that simulates the intracellular environment. We find that the methylome is remarkably static—over 95% of adenosine bases retain their methylation status across conditions. Integration of methylation with transcriptomic data revealed limited correlation between changes in methylation and gene expression. Further, examining the transcriptome in Δ*yhdJ* bacteria, lacking the $m^6A$ methylase with the most dynamic methylation pattern in our dataset, revealed little evidence of YhdJ-mediated gene regulation. Curiously, despite G($m^6A$)TC motifs being particularly resistant to change across conditions, incorporating *dam* mutants into our analyses revealed two examples where changes in methylation and transcription may be linked across conditions. This includes the novel finding that the Δ*metJ* motility defect may be partially driven by hypermethylation of the chemotaxis gene *tsr*. Together, these data redefine the *S.* Typhimurium epigenome as a highly stable system that has rare, but important, roles in transcriptional regulation. Incorporating these lessons into future studies will be critical as we progress through the epigenomic era.


## Importance

While recent breakthroughs have enabled intense study of bacterial DNA modifications, limitations in current work have potentiated a surprisingly untested narrative that DNA methylation is a common mechanism of the bacterial response to environmental conditions. Essentially, whether epigenetic regulation of bacterial transcription is a common, generalizable phenomenon is a critical unanswered question that we address here. We find that most DNA methylation is static in *Salmonella enterica* serovar Typhimurium, even when the bacteria are grown under dramatically different conditions that cause broad changes in the transcriptome. Further, even when the methylation of individual bases change, these changes generally do not correlate with changes in gene expression. Finally, we demonstrate methods by which data can be stratified in order to identify coupled changes in methylation and gene expression.

## Introduction

Until recently, systematically understanding how the bacterial DNA methylome affects physiology has been an unachievable task. Unlike eukaryotes where $m^5C$ DNA methylation is highly abundant and can be detected with bisulfate sequencing (1), bacterial genomes primarily house $m^6A$ methylation which has historically been difficult to detect. Despite this technological hurdle, many studies over the last several decades have successfully uncovered roles for DNA methylation both in the contexts of restriction-modification systems (reviewed (2)), as well as for "orphan" methylases (particularly the Dam methylase) in DNA repair (3-9), DNA/bacterial replication and viability (10-19), *agn43* phase variation (20), LPS modifications (21-25), phage defense (21,26,27), mating (28,29), fimbriae formation (30,31), antibiotic resistance (32), hypoxia survival (33), motility (17,23,31,34), and other virulence related processes (8-10,16-19,23,31,34-39). While orphan methylases were originally thought to regulate bacterial physiology while restriction-modification systems targeted foreign DNA, recent work on "phasevarions" have found restriction-modification systems can indeed have dramatic impacts on the genome (reviewed (40)).

83 A more complete history of associations between methylases and phenotypes can be found in
84 recent reviews (41-43).
85 While early epigenome studies are valuable for the insights they provide, they depended
86 on low-throughput and relatively blunt approaches (*e.g.,* restriction enzyme digests paired with
87 southern blotting to infer methylation). These approaches could not be leveraged to address if and
88 how genome-wide changes in DNA methylation associate with changes to cellular processes.
89 However, the discovery that sequencing data from the Pac-Bio SMRT-sequencing (44) and Oxford
90 Nanopore sequencing (45,46) systems can be repurposed to detect $m^6A$ has heralded a golden age
91 of bacterial DNA methylomics. These technological breakthroughs were rapidly applied to
92 cataloging bacterial methylomes, many of which have been deposited in publicly available
93 databases such as REBASE (47). However, we have only recently seen the power of these third-
94 generation sequencing technologies applied to connect DNA methylation to cellular phenotypes.
95 For instance, a recent paper utilized SMRT-seq to identify specific changes in G($m^6A$)TC patterns
96 within the *opvAB* promoter that are highly present in the population following phage insult (48),
97 building on previous phenotypic observations (21). Other groups have leveraged comparative
98 epigenomics to examine methylation patterns across isolates and identify potentially important
99 trends in methylation (35,49,50). Thus, there is immense potential for SMRT-seq to identify how
100 methylation correlates with impactful biology.
101 Despite these advances we note that few studies have leveraged SMRT-seq to understand
102 how methylation itself changes under different environmental pressures. Instead, the studies listed
103 above typically examine methylomes under a single condition (typically late stationary-phase
104 growth) to infer where methylation *can* happen, with notable exception (11,32,51-53). While
105 informative, these approaches may not represent the methylation status of bacteria at growth
106 phases typically studied in bacteriology, and thus may have limited ability to integrate into the
107 broader microbiological literature and with transcriptomic datasets. A related shortcoming of many
108 methylation studies is that methylation sites in promoters are often reported as evidence of
109 methylation-mediated regulation, without determining whether methylation is dynamic under
110 relevant environmental changes or testing whether disrupting methylation at those sites impacts
111 transcription. Curiously, while a number of classical approaches have identified examples of
112 methylation at specific sites regulating gene expression (*e.g. pap* (30,54,55), *opvAB* (21), *agn43*
113 (56,57), *gtr* (22), the *std* operons (58), *dnaA* (12), *traJ* (29), and *sci1* (36)), we are unaware of any
114 methylation site originally identified using genome-wide approaches that has been confirmed to
115 impact gene expression. This disconnect between the technological advances in methylomics and
116 the relatively modest conceptual advances in the field make it clear that the use of third generation
117 sequencing technologies to interrogate the DNA methylome is still in its infancy and that the
118 important question of the generalizability of epigenetic regulation of transcription in bacteria
119 should be addressed.
120 In this paper, we perform a series of SMRT-seq and RNA-seq experiments to understand
121 the role of DNA methylation in regulating *Salmonella enterica* serovar Typhimurium (*S.*
122 Typhimurium) gene expression under environmental conditions critical for *Salmonella* virulence.
123 Specifically, we studied conditions that activate the motility and *Salmonella* Pathogenicity Island-
124 1 (SPI-1) pathways (growth in LB until late-log phase) and conditions that activate the *Salmonella*
125 Pathogenicity Island-2 (SPI-2) pathways (growth in LPM media (59) until late-log phase). As
126 methionine metabolism is intimately connected to methylation, we also examined the changes in
127 methylation associated with derepressed methionine metabolism using a Δ*metJ* mutant. In general,
128 we find that DNA methylation is mostly stable across conditions and is broadly decoupled from

129 gene expression changes. This work redefines our understanding of the *S.* Typhimurium
130 epigenome, provides multiple epigenomic datasets that can be incorporated into future work to
131 identify rare instances where methylation changes are coupled with transcription, and a basic
132 blueprint for carrying out future methylomic studies with high reproducibility.
133
134 **Materials and Methods**
135 Bacterial cell culture
136 All *Salmonella* strains are derived from *S.* Typhimurium NCTC 12023 (ATCC 14028s)
137 and are included in **Supplemental Table 1**. All plasmids are included in **Supplemental Table 2**.
138 Chromosomal knockouts were generated by lambda-red recombineering (60). Site-directed
139 mutagenesis of the chromosome was performed using a modified version of lambda-red
140 recombineering, as previously described (61). Complementation plasmids were generated by cut
141 and paste cloning using the pWSK129 plasmid (62). For all experiments, bacteria were maintained
142 on LB (BD, Miller formulation) agar plates, grown in LB media overnight at 37°C at 250 RPM,
143 and subcultured the following morning prior to experiments. The SPI-2 inducing media is the low
144 phosphate and magnesium (LPM) media from Coombes *et al*. (59) and contains 5 mM KCl,
145 7.5mM $(NH_4)_2SO_4$, 0.5mM $K_2SO_4$, 38mM glycerol (0.3% volume/volume), 0.1% casein
146 hydrolysate, 8μM $MgCl_2$, 337μM $K_2HPO_4$ (pH 5.8), 80mM MES (pH 5.8), with the final solution
147 pH equal to 5.8. Propagation of temperature sensitive plasmids occurred at 30˚C and were cured
148 at 42˚C. Ampicillin was added to media at 100 μg/mL, kanamycin at 50 μg/mL, and apramycin at
149 100 μg/mL.
150
151 Mammalian cell culture
152 THP-1 monocytes from the Duke Cell Culture Facility were cultured at 37°C in 5% CO2
153 in RPMI 1650 media (Invitrogen) supplemented with 10% heat-inactivated FBS, 2μM glutamine,
154 100 U/mL penicillin-G, and 100 mg/mL streptomycin. Cells used for *Salmonella* gentamicin
155 protection assays were grown in antibiotic free media one hour prior to infection.
156
157 Sample preparation for SMRT-Seq
158 *S.* Typhimurium were grown overnight, washed once, and subcultured 1:33 in LB for 2
159 hours and 45 minutes to induce SPI-1 expression, or 1:50 in SPI-2 inducing media for 4 hours in
160 order to induce SPI-2 expression. $2x10^9$ bacteria were pelleted and DNA was extracted using a
161 DNeasy Blood and Tissue kit (Qiagen). The optional RNase step in the protocol was performed to
162 remove contaminating RNA, per manufacturer instructions. DNA was stored at 4˚C until library
163 preparation. Multiplexed SMRTbell libraries for sequencing on the PacBio Sequel system were
164 prepared from 1 μg of each microbial gDNA sample. Shearing of gDNA was performed using g-
165 TUBE and centrifugation at 2029 x g for 2 minutes to achieve a target mode size of 10 kb - 15 kb.
166 SMRTbell libraries were then prepared using the SMRTbell Express Template Prep Kit 2.0. Two
167 pools of 8 indexed libraries were prepared. Each pool was then sequenced on a PacBio Sequel
168 SMRTcell using sequencing chemistry 3.0 and 10 hour movie length.
169
170 Sample preparation for RNA-Seq
171 *S.* Typhimurium were grown overnight, washed once, and subcultured 1:33 in LB for 2 hours and
172 45 minutes, or 1:50 in SPI-2 inducing media for 4 hours. $2x10^9$ bacteria were pelleted at 5,000 x g
173 for 5 minutes, and resuspended in RNAprotect Bacteria Reagent (Qiagen) in order to stabilize
174 transcripts. After 5 minutes, bacteria were re-pelleted, and resuspended in 200 μL of TE Buffer

175 containing lysozyme (15 mg/mL) and 20µL of Proteinase K. Bacteria were vortexed every two
176 minutes for 15 minutes. 700 µL of β-mercaptoethanol-containing RLT buffer was added. After
177 vortexing, 500 µL of 96% ethanol was added, and the solution was mixed and applied to a RNeasy
178 extraction column (Qiagen). The remainder of the RNeasy protocol was followed per manufacturer
179 instructions. After RNA isolation, 3-6 µg of RNA was treated with Turbo DNase (Thermo-Fisher)
180 per manufacturer instructions, with the exception that two successive 30-minute DNase treatments
181 were performed. To remove DNase after treatment, the solution was mixed with 350 µL of β-
182 mercaptoethanol-containing RLT buffer, and then 700 µL of 96% ethanol was added. The mixture
183 was then added to a RNeasy MinElute column (Qiagen) and RNA was reisolated according to
184 manufacturer instructions.
185 RNA samples QC was performed with an Agilent Fragment Analyzer and a Qubit assay
186 on the PerkinElmer Victor X2. Illumina TruSeq Stranded total RNA-Seq Kit combined with Ribo-
187 Zero rRNA removal kit (bacteria) was used to prepare total RNA-seq libraries. Total RNA was
188 first depleted of the rRNA using biotinylated probes that selectively bind to rRNA molecules. The
189 rRNA depleted RNA was then reverse transcribed. During the 2nd strand synthesis, the
190 cDNA:RNA hybrid is converted into to double-stranded cDNA (dscDNA) and dUTP incorporated
191 into the 2nd cDNA strand, effectively marking the second strand. Illumina sequencing adapters
192 were then ligated to the dscDNA fragments and amplified to produce the final RNA-seq library.
193 The strand marked with dUTP is not amplified, allowing strand-specificity sequencing. Libraries
194 were indexed using a dual indexing approach allowing for multiple libraries to be pooled and
195 sequenced on the same sequencing flow cell of an Illumina MiSeq sequencing platform. Before
196 pooling and sequencing, fragment length distribution and library quality was first assessed on a
197 Fragment Analyzer using the High Sensitivity DNA Kit (Agilent Technologies). All libraries were
198 then pooled in equimolar ratio and sequenced. Sequencing was done at 50 bp single-end reads.
199 Once generated, sequence data was demultiplexed and Fastq files generated using Bcl2Fastq
200 conversion software from Illumina.
201
202 SMRT-seq mapping and $m^6A$ analysis
203 $m^6A$ methylation calls were performed using the pbsmrtpipe base modification and motif
204 detection pipeline (Smrtlink v7.0.1.66975) with *Salmonella enterica* serovar Typhimurium strain
205 14028s (ASM2216v1) as the reference genome. For sites at or above 50x coverage, sites with a
206 phred-based quality score greater than 40 were marked as "1", for strong evidence of methylation;
207 sites with >=50x coverage but below QV40 were marked as "0", for unlikely to be methylated.
208 For sites below 50x coverage, methylation status was not estimated. Assigning methylated bases
209 to motif(s) was performed by comparing the context of the base to known or identified motifs
210 using Microsoft Excel. Motif enrichment was calculated by dividing the frequency of the motif in
211 a given subset (*e.g.* frequency of the motif in bases only methylated in bacteria grown in LB) and
212 dividing by the frequency of the motif in condition tested (*e.g.* frequency of the motif among all
213 methylated bases in bacteria grown in LB). Additional methyl-bases were detected on the pWSK29
214 plasmid harbored in these strains; however, we did not include these bases in our analyses as this
215 plasmid is not involved in the natural lifestyle of *S.* Typhimurium.
216
217 RNA-seq analysis and integration with methylomics
218 RNA-seq data was processed using the TrimGalore toolkit
219 (http://www.bioinformatics.babraham.ac.uk/projects/trim_galore) which employs Cutadapt (63)
220 to trim low quality bases and Illumina sequencing adapters from the 3' end of the reads. Only reads

221 that were 20 nt or longer after trimming were kept for further analysis. Reads were mapped to the
222 ASM2216v1 version of the *Salmonella enterica* strain 14028S genome and transcriptome (64)
223 using the STAR RNA-seq alignment tool (65). Reads were kept for subsequent analysis if they
224 mapped to a single genomic location. Gene counts were compiled using the HTSeq tool
225 (http://www-huber.embl.de/users/anders/HTSeq/). Only genes that had at least 10 reads in any
226 given library were used in subsequent analysis. Normalization and differential expression was
227 carried out using the DESeq2 (66) Bioconductor (67) package with the R statistical programming
228 environment (https://www.R-project.org/).The false discovery rate was calculated to control for
229 multiple hypothesis testing.
230 Integration of methylomics and RNA-seq analysis occurred in three steps. First, a list of
231 genes present in both analyses was generated. Second, rates of differential expression among (a)
232 the entire list of genes present in both analyses and (b) differentially methylated genes were called
233 as genes containing 1+ base that was methylated in one condition but not another. Third, expected
234 (frequency of differential expression in the entire list of genes present in both analyses multiplied
235 by the frequency of differential methylation multiplied by the total number of genes in the analysis)
236 and observed differentially methylated and differentially expressed genes were compared. Fisher's
237 Exact Test was used to determine whether there were statistically significant associations between
238 differential methylation and differential expression.
239
240 Analysis of *yhdJ* across *Salmonella* genomes
241 In order to analyze conservation of *yhdJ* across the *Salmonella enterica* genomes, 9,078
242 genomes (1,000 Typhimurium, 1,000 Typhi, 1,000 Paratyphi A, 1,000 Paratyphi B, 999 Newport,
243 1,000 Dublin, 1,000 Enteritidis, 1,000 Agona, 1,000 Heidelberg, and 79 Derby genomes) were
244 obtained from the EnteroBase repository (68,69). Serovars examined here were specifically chosen
245 to test for conservation among a diverse group of *Salmonella*. The specific strains were randomly
246 selected and represented a variety of sources (human, agricultural animal, avian, reptiles,
247 environment, etc.) within serovars, when possible. After downloading the genomes, all genomes
248 of a given serovar were concatenated into a single FASTA file and used for analysis with the
249 BLAST+ command line software (70). The 14028s YhdJ protein sequence was used as query for
250 the pBLASTn program. To determine conservation, the program produced BLAST scores for 'n'
251 sequences, where n = the number of strains tested within each serovar. The BLAST scores were
252 then plotted relative to the BLAST score obtained using the 14028s genome.
253
254 GO-term analysis
255 All GO-terms were generated using the Gene Ontology Resource
256 (http://geneontology.org/) (71,72). The PANTHER Overrepresentation Test was run using the
257 *Salmonella* Typhimurium GO biological process reference, the test used Fisher's Exact test, and
258 the correction was based on a calculated false discovery rate. All calculations were run
259 automatically though the web portal software. Any gene that was not present in the GO-term
260 database was "unmapped" and excluded from the analysis.
261
262 Growth curves
263 *S.* Typhimurium were grown overnight in LB, subcultured 1:50 into 5mL of either LB or
264 SPI-2 inducing media, and grown at 37˚C at 250RPM. OD600 measurements were taken every 30
265 minutes using a spectrophotometer (Pharmacia Biotech Novaspec II).
266

267 Gentamicin protection assay
268 Invasion and replication were measured as previously described (73-75). Briefly, bacteria
269 were grown overnight, subcultured 1:33 into 1mL of LB, and grown for 2 hours and 45 minutes
270 or until all strains entered late-log phase growth (OD600=1.5-2.0) at 37˚C with 250 RPM. For any
271 experiment using Δ*dam* bacteria, all bacteria were grown an extra 30 minutes (3 hours and 15
272 minutes) so that the Δ*dam* and Δ*dam*Δ*metJ* mutants reached late-exponential phase growth.
273 100,000 THP-1 monocytes, in antibiotic free media, were then infected by *S.* Typhimurium (MOI
274 5). At one hour post infection, cells were treated with gentamicin (50μg/mL), and IPTG was added
275 2 hours post infection to induce bacterial GFP expression. At 3 hours and 15 minutes post infection,
276 cells were read by a Guava Easycyte Plus flow cytometer (Millipore). At 22 hours and 45 minutes
277 post infection, IPTG was added to remaining wells to induce GFP, and at 24 hours post infection,
278 cells were quantified by flow cytometry. Percent host cell invasion was determined by quantifying
279 the number of GFP+ cells 3 hours and 15 minutes post infection, and replication was assessed by
280 determining the ratio of the median intensity of GFP positive cells at 24 hours post infection
281 divided by the median of the GFP positive cells at 3 hours and 15 minutes post infection.
282
283 Motility assays
284 All strains were cultured overnight in LB, subcultured 1:33 into LB, and grown for 2 hours
285 and 45 minutes at 37˚C with 250 RPM. A pipette tip was used to puncture and deliver 2μL of *S.*
286 Typhimurium into the center of a 0.3% LB agar plate. Plates were incubated at 37°C for 6 hours
287 before the halo diameter was quantified.
288
289 Murine competitive index experiments
290 Mouse studies were approved by the Duke Institutional Animal Care and Use Committee
291 and adhere to the *Guide for the Care and Use of Laboratory Animals* of the National Institutes of
292 Health. All experiments were performed with age- and sex-matched C57BL/6J (7-14 weeks old)
293 mice. Bacteria were grown overnight, subcultured 1:33, and grown for 2 hours and 45 minutes at
294 37˚C with 250 RPM. The bacteria were then washed and resuspended in PBS. Inoculums were
295 confirmed by plating for CFUs. For oral infections, mice were fasted for 12 hours before infection,
296 and given 100 μL of a 10% sodium bicarbonate solution by oral gavage 30 minutes before
297 infection. Mice then received a 1:1 mixture of two *S.* Typhimurium strains containing either
298 pWSK29 (AmpR) or pWSK129 (KanR) (62), totaling $10^8$ CFU in 100μL, by oral gavage. For
299 intraperitoneal (IP) infections, mice were injected with a 1:1 mixture of two *S.* Typhimurium
300 strains, totaling $10^3$ CFU in 100uL, into the intraperitoneal space. For both models, tissues were
301 harvested four days post infection, homogenized, and plated on LB agar containing either
302 ampicillin or kanamycin. Competitive index was calculated as (# Strain A CFUs in tissue/# Strain
303 B CFUs in tissue)/ (# Strain A CFUs in inoculum/# Strain B CFUs in inoculum). Statistics were
304 calculated by log transforming this ratio from each mouse and comparing to an expected value of
305 0 using a one-sample t-test.
306
307 RT-qPCR
308 RNA was harvested as described above and used to create cDNA using the iScript cDNA
309 synthesis kit (Bio-Rad Laboratories). qPCR was performed using the iTaq Universal SYBR Green
310 Supermix (Bio-Rad Laboratories). 10 μL reactions contained 5 μL of the supermix, a final
311 concentration of 500 nM of each primer, and 2 μL of cDNA. Reactions were run on a QuantStudio
312 3 thermo cycler. The cycling conditions were as follows: 95°C for 30 seconds, 40 cycles of 95

313 degrees for 15 seconds and 60°C for 60 seconds, and 60°C for 60 seconds. A melt curve was
314 performed in order to verify single PCR products. The comparative threshold cycle ($C_T$) method
315 was used to quantify transcripts, with the ribosomal *rrs* gene serving as the endogenous control.
316 Fold change represents $2^{-\Delta\Delta CT}$. Oligonucleotides are listed in **Supplemental Table 3**.
317
318 Western blotting
319 *flhC* was tagged with the 3xFLAG tag using recombineering as previously described (76).
320 *S.* Typhimurium were grown overnight in LB, subcultured 1:33 in LB at 37˚C with 250 RPM until
321 late log phase (OD600-1.5-2.0), and pelleted by centrifugation at 6,000 x g for 5 minutes. Pellets
322 were resuspended in 2x laemmli buffer (Bio-Rad) with 5% 2-Mercaptoethanol, boiled for 10
323 minutes, and lysates were run on Mini-PROTEAN TGX Stain-Free gels (Bio-Rad). After
324 electrophoresis the gels' total protein dye was activated by a 5-minute UV exposure. Following
325 transfer onto Immun-Blot low-fluorescence PVDF membrane (Bio-Rad) using a Hoefer TE77X,
326 blots were probed using an anti-FLAG M2 antibody (Sigma F3165). A florescent secondary
327 antibody (LI-COR IRDye) was used to detect bands on a LI-COR Odyssey Classic. Band intensity
328 was quantified using LI-COR Odyssey Imaging System Software v3.0. Total protein was detected
329 by 30 seconds of UV exposure, and quantified using Fiji (77). The graphed relative signal is:
330 (FLAG band intensity/Total Protein) divided by (FLAG band intensity in wild-type *flhC:FLAG3x*
331 bacteria/Total Protein in wild-type *flhC:FLAG3x* bacteria).
332
333 Statistical analyses
334 Statistics were performed in Graphpad Prism 9 or Microsoft Excel, except where otherwise
335 noted. Where noted, inter-experimental noise was removed from gentamicin protection assays and
336 motility assays prior to data visualization or statistical analysis by standardizing data to the grand
337 mean by multiplying values within an experiment by a constant (average of all experiments divided
338 by average of specific experiment). All statistical tests corresponding to reported p-values are
339 described in the appropriate figure legends.
340
341 **Results**
342 **A genome-wide screen to understand how growth conditions and methionine metabolism**
343 **impact m$^6$A DNA methylation**
344 While previous work on bacterial DNA methylation has largely focused either on global
345 DNA methylation patterns under a single condition or on how methylation of a single motif
346 changes under different conditions, we sought to examine how the entire *S.* Typhimurium m$^6$A
347 DNA methylome changes under four biologically relevant conditions **(Figure 1A)**. We examined
348 aerobic growth in LB media to late exponential phase (OD600 ~1.5-2.0), which induces expression
349 of flagellar genes and the genes in the *Salmonella* Pathogenicity Island-1 (SPI-1)—including the
350 type III secretion system used during host cell invasion (78). The second condition cultured
351 bacteria in a minimal media used to induce expression of genes in the *Salmonella* Pathogenicity
352 Island-2 (SPI-2) (59)—which include the type III secretion system turned on in the host cell to
353 promote *Salmonella* vacuolar survival (79,80). The third and fourth conditions repeated growth in
354 these media but used a methionine metabolism mutant *S.* Typhimurium strain, Δ*metJ*. The MetJ
355 protein represses expression of methionine metabolism genes (81). Thus, Δ*metJ* bacteria have
356 deregulated methionine metabolism, and accumulation of methionine and related metabolites,
357 including metabolites directly related to methylation processes such as the universal methyl-donor
358 S-adenosyl-methionine (SAM) (82), and the methyltransferase-inhibiting metabolites

359 methylthioadenosine (83-85) and S-adenosyl-homocysteine (86-90). Of note, we have not only
360 previously confirmed increased abundances of both SAM and MTA in Δ*metJ*, but also
361 demonstrated that the Δ*metJ* mutant has attenuated SPI-1 secretion, motility, and virulence (91)
362 and had previously hypothesized that these effects could be mediated through aberrant
363 methylation.
364 To analyze the DNA methylome, we performed a PacBio SMRT-sequencing experiment
365 (hereon called "Methylation Experiment 1") in biological singlet (as has been common in the field
366 and as we comment on below) to identify whether any changes in methylation could be observed.
367 In this experiment, we also included Δ*dam* and Δ*dam*Δ*metJ* mutants, which lack G($m^6$A)TC
368 (henceforth the * symbol will denote the adenosine that is $m^6$A modified; GA*TC) methylation
369 grown under SPI-1 and SPI-2 conditions. This allowed us to confirm that our pipeline could
370 adequately detect changes in methylation. These eight conditions were split across two PacBio
371 SMRT Cells. Thus, these conditions enabled comparison of the *S.* Typhimurium DNA methylome
372 under the two conditions most critical for *Salmonella* virulence, under perturbation of methionine
373 metabolism, and with a control condition ablating the primary DNA methyltransferase.
374 In total this experiment defined the methylation status of 61,704 adenosine bases **(GEO:**
375 **GSE185578)**, however, methylation status of some bases under certain conditions could not be
376 determined as coverage was below 50X. Thus, we restricted our analysis to 51,177 bases in which
377 the methylation status could be adequately determined for all conditions tested. These bases span
378 both the *S.* Typhimurium genome and virulence plasmid.
379 To compare methylation across conditions, we called methylation in two ways. First, we
380 assigned each base a "percent methylated" value, which considered the percent of reads for each
381 base that were counted as methylated compared to the total number of reads **(Supplemental File**
382 **1)**. We also examined the data as a binary in which we considered bases either methylated (if any
383 methylation was detected) or unmethylated **(Supplemental File 2)**. Using this binary analysis, we
384 observed that there were similar, but subtly different, amounts of $m^6$A methylation across wild-
385 type and Δ*metJ* bacteria grown in LB and SPI-2 conditions (WT LB: 39,240 bases; WT SPI-2:
386 38,827 bases; Δ*metJ* SPI-1: 39,352 bases; Δ*metJ* SPI-2: 40,145 bases) **(Figure 1B)**, but that, as
387 expected, Δ*dam* reduced total methylation substantially **(Figure 1C)**.
388
389 **ATGCAT motifs are frequently differentially methylated across conditions**
390 We next examined how these bases were distributed across different methylation motifs.
391 This analysis detected methylation at motifs that had been previously detected in *S.* Typhimurium
392 (92), though we were able to detect an additional motif, CRTA*$YN_6$CTC, which appears to be the
393 reverse complement of GA*$GN_6$RTAYG. Notably, two motifs (CAGA*G and GA*$GN_6$RTAYG)
394 cannot always be distinguished, and so we included bases that matched to both motifs in counts
395 for each. Bases that did not map to any known motif were listed as "Other." As with the total
396 amount of $m^6$A methylation, we found that our four main conditions had subtle differences in the
397 total numbers of most motifs **(Figure 1D)**.
398 The most notable change in motif abundance occurred at the ATGCA*T motif, which is
399 methylated by the YhdJ methylase (93). We observed more ATGCA*T methylation in bacteria
400 grown under SPI-2-inducing conditions ($p<0.00001$, Chi-Square Test) or in Δ*metJ* bacteria
401 ($p<0.00001$, Chi-Square Test), with the highest ATGCA*T methylation present in Δ*metJ* bacteria
402 grown under SPI-2-inducing conditions. We also observed variation in the number of bases that
403 mapped to the "Other" category. In contrast, we observed very little change in the total amount of
404 GA*TC methylation (methylated by Dam) across these physiologically relevant conditions,

405 though deletion of *dam* resulted in almost complete ablation of methylation at the GATC motif
406 **(Figure 1E)**.
407 To examine the methylation changes under LB vs. SPI-2 inducing conditions with wild-
408 type and Δ*metJ S.* Typhimurium, we compared binary methylation at each individual base to
409 identify differentially methylated bases (bases that were called methylated in one condition but not
410 another). While each condition had a few hundred to over a thousand bases that were not
411 methylated in their opposing group, the vast majority of bases in this study (>38,000) were shared
412 across these comparisons **(Figure 2A, 2B, 2C; Venn Diagrams)**. This demonstrates that while the
413 methylome is slightly responsive to the environment and methionine metabolism, it remains
414 largely static across strikingly different conditions.
415 Having identified these differentially methylated bases by our binary analyses, we
416 integrated our quantitative data. This is an important measurement as previous work has speculated
417 that methylation impacts bistable gene expression (48,94), and thus changes in the percent of the
418 population in which a given base is methylated could have implications on the percent of the
419 population expressing a given gene. For each differentially methylated base, we asked what the
420 total change in methylation was across the two conditions **(Figure 2A, 2B, 2C; Graphs)**. The total
421 median shift in the percent methylation varied by condition, but fell between 43% and 53%,
422 suggesting that most bases go from unmethylated in one condition, to about half the copies of the
423 genome having methylation at that site in the other. Notably, most of the "shared" bases that
424 demonstrated methylation under both conditions demonstrated no quantitative change (median =
425 0%). However, again the exception was ATGCA*T, where the median shift among shared bases
426 remained relatively high (11-23% depending on condition).
427 To test for enrichment of motifs among differentially methylated bases, we compared the
428 frequency of each of the six motifs tested above in the differentially methylated sites against the
429 frequency observed in the entire condition. This analysis revealed that among the uniquely SPI-2-
430 induced methylated bases, we observed 37 times more differentially methylated ATGCA*T sites
431 than expected. Similarly, sites methylated in Δ*metJ S.* Typhimurium, but not wild-type bacteria,
432 grown under both LB and SPI-2-inducing conditions are also dramatically enriched for YhdJ-
433 mediated methylation (20-fold and 11-fold enrichment, accordingly) **(Supplemental Figure 1)**.
434 Surprisingly, all other motifs were either present at similar or dramatically lower abundance among
435 differentially methylated sites than expected by chance, though we did note significant enrichment
436 of "other" motifs among differentially methylated bases (20 to 100-fold enrichment, depending on
437 condition).
438
439 **A replication experiment demonstrates that SMRT-seq is highly reproducible and confirms**
440 **differential methylation is predominantly driven by YhdJ**
441 To confirm our findings that DNA methylation was largely stable among our conditions
442 with the exception of ATGCA*T sites, we repeated our SMRT-seq experiment with wild-type and
443 Δ*metJ* bacteria grown in LB **(Supplemental Figure 2A;** Replication Methylation Experiment**)**.
444 Further, to confirm that the significant enrichment in ATGCA*T methylation in Δ*metJ* bacteria
445 we observed above was due to YhdJ, we also sequenced Δ*yhdJ* and Δ*yhdJ*Δ*metJ S.* Typhimurium
446 grown in LB. Of note, while we sequenced eight samples across two SMRT cells in Methylation
447 Experiment 1, here we sequenced these four samples on two SMRT cells, significantly increasing
448 our sequencing depth. The resulting dataset called the methylation status of 60,502 bases in at least
449 one condition, and, strikingly, 60,501 of these bases were confidently called in all four conditions
450 **(GEO: GSE185501**).

451 Analysis of the two methylomic datasets using our binary assessment revealed that ~97.5%
452 of bases replicated their methylation status across experiments, demonstrating that our results were
453 highly reproducible **(Supplemental Figure 2B, Supplemental File 2)**. Importantly, we again
454 observed that Δ*metJ* bacteria have increased ATGCA*T methylation and found 0 methylated
455 ATGCA*T sites in the Δ*yhdJ* and Δ*yhdJ*Δ*metJ* mutants, confirming that YhdJ is the only
456 ATGCA*T methylase active in both bacterial strains **(Supplemental Figure 2C)**. Of note, sites
457 assigned to "other" motifs may include significantly more miscalled methyl bases, as only ~80%
458 (79.3% of wild-type and 80.1% of Δ*metJ*) "other" bases replicated their methylation status across
459 experiments.
460 Analysis of the two datasets using the quantitative measurement **(Supplemental File 3)**
461 revealed considerable replication across the datasets (wild-type $R^2$=0.87 and Δ*metJ* $R^2$=0.86)
462 **(Supplemental Figure 2D)**. Considering these experiments as separate biological replicates and
463 using an arbitrary cutoff of 10% average differential methylation, we identified 2,528 sites (out of
464 50,962 total sites; 4.96%) that were differentially methylated between wild-type and Δ*metJ*
465 bacteria using this quantitative method (**Supplemental Figure 2E)**. 881 of these sites were more
466 methylated in wild-type bacteria, and 1,647 were more methylated in Δ*metJ* bacteria.
467 Having assessed the reproducibility of SMRT-Seq for both categorical and quantitative
468 measures of methylation, we used our binary measurement to generate a combined dataset
469 containing bases which were (a) reliably detected in wild-type and Δ*metJ* bacteria grown in LB in
470 both experiments, and (b) were identically called methylated or unmethylated in both experiments.
471 Using this dataset (52,594 bases), we determined which differentially methylated bases repeated
472 across the two studies. This number of bases is greater than the number of bases included in
473 Methylation Experiment 1 analyses, as we no longer needed to exclude bases that did not reach
474 sufficient coverage in either the SPI-2 inducing or Δ*dam* conditions. While our data demonstrated
475 that the vast majority of bases were called identically (~97.5%; **Supplemental Figure 2B)**, we
476 found that a disproportional number of bases that were called differentially methylated in the pilot
477 study failed to replicate in the replication study, and vice versa. In fact, while there were 1,382
478 bases called differentially methylated in the first experiment **(Figure 2B)**, and 2,544 bases called
479 differentially methylated in the replicate study **(Supplemental Figure 2F)**, only 308 differentially
480 methylated bases were identified in the combined dataset (**Supplemental Figure 2G)**.
481 Importantly, the overlap between these two replicates is much greater than expected by chance
482 (3.7-fold enrichment; $p<0.0001$, one-tailed binomial test), indicating that these biological
483 replicates provide a high-confidence set of 308 differentially methylated sites, though some false
484 positives likely remain. Our findings emphasize that while SMRT-seq calling of methylated bases
485 is reliable, replication is especially important in examining bases that change between conditions.
486 Of note, the combined dataset once again revealed enrichment of differentially methylated
487 "other" sites. To understand these sites, we examined the 40 bases surrounding the 143 instances
488 of "other" differential methylation in the Combined Dataset using the Multiple Em for Motif
489 Elicitation (MEME) software (95). This identified a single significant motif (E-value=$6.1 \times 10^{-16}$),
490 ACCWGG **(Supplemental Figure 3A)**. The same motif was identified among the 969
491 differentially methylated "other" sites between LB and SPI-2 grown bacteria (Methylation
492 Experiment 1; E-value = $5.5 \times 10^{-206}$; **Supplemental Figure 3B**). The ACCTGG motif has been
493 reported on multiple *Salmonella* serovar entry pages on REBASE (47), however, curators note that
494 this is almost certainly a miscall for the $m^5C$ motif CCWGG—methylated by Dcm. Across the
495 combined dataset, we found 33 instances of this motif (23% of all differentially methylated "other"
496 sites). This leads us to hypothesize that this dynamic "other" category may be predominantly

497 driven by changes in the flexible $m^5C$ methylome, which warrants further investigation using
498 sequencing technologies better equipped to detect cytosine methylation.
499
500 **There is no association between the transcriptome and the genome-wide binary methylation**
501 **analyses under the conditions tested here**
502 Canonically, changes in DNA methylation can lead to changes in transcription by enabling
503 differential binding of transcription factors to genomic elements (reviewed (41)). However, studies
504 that describe this in bacteria typically either (a) focus on single loci (for example, (48)), or (b) only
505 speculate on direct mechanisms of transcriptional control based on methylase knockout
506 experiments (for example (35)). No study has directly examined whether differential methylation
507 across the *S.* Typhimurium genome correlates with differential expression under biologically
508 relevant conditions. We attempted to fill this gap in knowledge by performing RNA-seq on wild-
509 type and Δ*metJ* bacteria grown in LB and SPI-2 inducing media **(GEO: GSE185072,**
510 **Supplemental File 4)** and looking for correlations with our SMRT-seq datasets.
511 Prior to integrating our datasets, we confirmed our RNA-seq data matched previously
512 observed trends. As expected, we identified many differentially expressed genes (2,639 DEGs at
513 FDR < 0.5) between wild-type bacteria grown in LB vs. SPI-2-inducing conditions **(Figure 3A)**.
514 These DEGs included a variety of expected genes, including higher expression of SPI-1genes (*e.g.,*
515 *sipB,* 322-fold induction) and flagellar genes (*e.g., fliD,* 138-fold induction) in LB and higher
516 expression of SPI-2 genes (*e.g., ssaN, sscA;* 182- and 579-fold induction respectively) in SPI-2
517 inducing media. Further, these data cluster with previous transcriptomic analyses of gene
518 expression in LB and SPI-2 inducing conditions (96) by PCA (53.5% of variation between the two
519 studies explained by media, **Supplemental Figure 4**). Analysis of Δ*metJ* DEGs revealed a number
520 of expected trends, specifically that during growth in LB and SPI-2, Δ*metJ* shows upregulation of
521 methionine metabolism genes resulting from direct derepression of the metabolic pathway **(Figure**
522 **3B, 3C)** (81). Of note, we also observed reduced motility gene expression which we had previously
523 reported (91), but were surprised that contrary to our prior work we observed a small reduction in
524 *flhD* expression in Δ*metJ*. However, we confirmed this result by qPCR and western blotting
525 **(Supplemental Figure 5A, 5B)**, and speculate that improved DNase treatment in this study likely
526 explains this difference.
527 To integrate our differential expression data with our methylomics data, we considered
528 genes that either (a) contained or (b) were the closest gene to one or more binary differentially
529 methylated sites (*ie.,* present at any level in one condition, absent in the other) to be "differentially
530 methylated genes" (DMGs) **(Figure 3D)**. For each comparison, the status "differentially
531 methylated" applied to the condition in which the methyl mark was present (*e.g.* when comparing
532 LB grown vs SPI-2 grown bacteria, an LB-grown DMG contains a methyl mark that is absent in
533 SPI-2 media grown bacteria). Using these criteria, we examined whether differentially methylated
534 genes were more likely to be differentially expressed than predicted by chance. Strikingly, we did
535 not observe enrichment of DEGs among our DMGs. The number of DEGs that were also DMGs
536 under all comparisons was remarkably similar to the overlap of these categories expected by
537 chance (Fisher's p-value > 0.05 in all cases), suggesting the two phenomena are typically not
538 associated at the genome-wide level across any of our comparisons with binary calling of DMGs
539 (**Figure 3E-G)**. Most importantly, there was no evidence of enrichment comparing WT *S.*
540 Typhimurium grown in LB (SPI-1 inducing) and SPI-2 conditions (**Figure 3E**), indicating that co-
541 occurrence of differential methylation and differential gene expression is not observed more
542 frequently than is expected by chance in switching between these two critical growth conditions
543 in *Salmonella* pathogenesis. Notably, we also did not observe correlations if we adjusted the

544 statistical thresholds for differential expression (**Supplemental Figure 6A-D**), or if we stratified
545 our data by the differential expression direction of effect **(Supplemental Figure 6E, 6F)**, the genic
546 location of the differential methylation **(Supplemental Figure 6G)**, or to specific motifs
547 **(Supplemental Figure 6H, 6I)**.
548
549 **There is limited association between the transcriptome and the genome-wide quantitative**
550 **methylation analyses under the conditions tested here**
551 In addition to these binary definitions to differential methylation, we examined whether
552 there was enrichment of DEGs among DMGs defined by a difference in ≥10% methylation across
553 conditions **(Figure 4A)**. Most of our binary observations replicated in this analysis **(Figure 4B,**
554 **4C)**, but we noted an association between DEGs and DMGs in wild-type bacteria grown in SPI-2
555 inducing media compared to Δ*metJ* bacteria grown in the same conditions **(Figure 4D, Table 1)**.
556 It is unclear why this condition is the exception to the general lack of association we observe, but
557 it may suggest that methylases (particularly the *dam* methylase) and deregulated transcriptional
558 machinery uniquely compete for access to these sites exclusively in minimal media. We also
559 examined whether adjusting our thresholds for differential expression or limiting our search for
560 differential to bases upstream of differentially expressed genes could reveal further correlations
561 between expression and methylation, but no additional associations were found **(Supplemental**
562 **Figure 7A-F)**. The association with sites in wild-type bacteria in SPI-2 media compared to Δ*metJ*
563 was still present with the more stringent DEG cutoff **(Supplemental Figure 7C)** but was no longer
564 present when analysis was restricted to upstream bases **(Supplemental Figure 7F)**. Finally, we
565 leveraged the quantitative dataset to examine the relationship between DMGs and DEGs in which
566 DMGs are defined by bases completely methylated in one condition (≥99%) and hypomethylated
567 in the other (≤89%) (**Supplemental Figure 7G-I)**. This revealed no additional associations, but
568 the association with wild-type bacteria in SPI-2 media replicated once again. We conclude that for
569 the crucial switch between SPI-1 and SPI-2 virulence gene programs, there is no association
570 between $m^6A$ DNA methylation and transcriptional regulation but that specific mutants may show
571 an association.
572
573 **YhdJ plays little role in *Salmonella* physiology under standard conditions important for**
574 **virulence**
575 While our data do not support a broad, global correlation between differential methylation
576 and differential expression under most of our tested conditions, particularly comparing wild-type
577 bacteria grown in LB and SPI-2 inducing conditions, this does not rule out that there are discreet
578 examples where methylation and gene expression are causally linked in our datasets. We
579 hypothesized that such instances could be identified by combining our data on methylation and
580 transcriptional patterns under biologically relevant conditions with data from methylase knockout
581 mutants to reduce our search space to putative sites of regulation. We tested this hypothesis with
582 the YhdJ (the most dynamic methylase in our dataset) and Dam (the most well-studied DNA
583 methylase in *Salmonella*) mutants.
584 RNA-seq on wild-type and Δ*yhdJ* bacteria grown in LB or SPI-2 inducing conditions
585 **(GEO: GSE185073, Supplemental File 5)** revealed that knocking out *yhdJ* had almost no impact
586 on the transcriptome. Apart from *yhdJ* itself, only 12 genes were differentially expressed in LB
587 (**Figure 5A, Table 2)** despite loss of methylation at all 513 ATGCA*T sites (see **Supplemental**
588 **Figure 2C**), and no genes were differentially expressed under SPI-2 inducing conditions **(Figure**
589 **5B)**. Curiously, GO-analysis (71,72) demonstrated the differentially expressed genes are enriched

590 for de novo UMP biosynthetic processes (False Discovery Rate=$6.3x10^{-4}$) and de novo pyrimidine
591 nucleobase biosynthetic processes (False Discovery Rate=$8.31x10^{-4}$). However, examining these
592 genes further revealed that only two differentially expressed genes contained or were near an
593 ATGCAT sequence (*dppA* and *pyrB*), and only *dppA* was detected to house a methylated
594 ATGCA*T motif in our Replication Methylation Dataset **(Table 2)**, making the mechanism of this
595 differential expression unclear. In agreement with these findings, *yhdJ* deletion had little impact
596 on cellular or virulence phenotypes. Δ*yhdJ* had no effect on growth in LB or SPI-2 inducing media
597 **(Figure 5C,D)**, a subtle increase on the amount of observed THP-1 cell infection **(Figure 5E)**, no
598 effect on replication in THP-1 cells **(Figure 5F)**, no effect on motility **(Figure 5G)**, and had almost
599 no effect on fitness in intraperitoneal or enteric fever models of mouse infection—though a small
600 increase in the number of Δ*yhdJ* CFUs recovered from the spleen relative to wild-type following
601 oral gavage was observed **(Table 3)**. Across all phenotypes, no genetic interaction between *yhdJ*
602 and *metJ* was detected. Thus, YhdJ has very little impact on transcription or virulence associated
603 phenotypes, and if anything, modestly impairs *Salmonella* virulence.
604 These findings suggest that YhdJ is almost entirely dispensable under the conditions tested
605 here, despite methylating over 500 sites in the genome and methylation of its ATGCA*T motif
606 being the most dynamic under the conditions tested. We questioned whether YhdJ may play roles
607 outside of transcription, and whether its dynamic nature is incidental. Supporting this hypothesis,
608 an evolutionary analysis of over 9,000 strains from 10 serovars revealed that the methylase is
609 highly conserved, with the exception of *S.* Paratyphi A where most strains harbor a 151* truncation
610 **(Figure 5H)**. This conservation paired with our RNA-seq data suggests that YhdJ methylation is
611 likely important but is unlikely to play a large role in gene regulation.
612
613 **Integration of previous Δ*dam* literature with methylomics data reveals *stdA* hypomethylation**
614 **correlates with expression in LB**
615 After demonstrating that a Δ*yhdJ* mutant could not be leveraged to identify instances where
616 gene expression and methylation are linked, we turned to the Δ*dam* literature. Previous work on
617 *Salmonella* transcriptomics revealed 17 virulence genes (making up 11 operons) that are
618 differentially expressed between wild-type and Δ*dam S.* Typhimurium grown in LB to mid-
619 exponential phase (31). We hypothesized that these sites may show differential methylation and
620 expression between our LB and SPI-2 medias, as *Salmonella* deploy radically different virulence
621 programs across these conditions and many of these 17 virulence genes are known to be expressed
622 specifically under only one of these two conditions (14 of 17 were DEGs comparing these two
623 conditions in our data, and the remaining three (STM14_3654, *stdB*, and *stdC*) lacked high enough
624 expression to analyze). In order to test this hypothesis, we searched for GATC motifs upstream
625 (within 500bp) of the DEGs. Interestingly, 10/11 genes or operons we examined contain GATC
626 sites within 500bp upstream of these genes **(Table 4)**. However, only one gene (*stdA*) showed
627 evidence of differential methylation under physiological conditions. Interestingly, *stdA* is the only
628 one of these 11 genes/operons where methylation of its promoter has been extensively studied
629 (58,97). The three GATC sites had reduced methylation following growth in LB, however, each
630 was only hypomethylated on a single strand (**Figure 6A**). Interestingly, this hypomethylation
631 agrees with a previous report that Dam and transcription factors compete for binding to the *stdA*
632 promoter (58), as we also observed significantly higher expression of *stdA* in LB than in SPI-2
633 media **(Figure 6B)**. Whether this represents a mechanism by which *stdA* is turned off in SPI-2
634 media or is a correlated consequence of increased *stdA* transcription in LB (or vice versa) is
635 unclear, but this finding demonstrates that the phenomenon that García-Pastor *et al*. describe in
636 Δ*dam* mutants occurs naturally under biologically relevant conditions. For the other 10 virulence

637 genes/operons that are reported to undergo differential gene expression in the *dam* mutant, we find
638 no evidence that differential methylation plays any role during their induction during SPI-1 or SPI-
639 2-inducing conditions.
640 We also attempted to integrate our data with a recent study that examined genetic
641 heterogeneity in *S.* Typhimurium (98). We examined the 16 hypomethylated sites they identified
642 to determine whether our dataset could find the same signatures of hypomethylation. Of the seven
643 sites we were able to find in our dataset, four showed signs of hypomethylation (**Supplemental**
644 **Table 4**). Of these four, two sites upstream of *carA* and *dgoR* showed differential methylation
645 across our conditions, however, no consistent trends were observed with differential gene
646 expression across our two RNA-seq datasets **(Supplemental Figure 8)**. Thus, while we were able
647 to observe an association of gene expression and DNA methylation for one canonical example
648 (*stdA*) during growth in LB vs. SPI-2 inducing conditions, we did not find this to be a generalizable
649 phenomenon for other genes reported to be differentially regulated in the *dam* mutant or
650 hypomethylated in *S.* Typhimurium.
651
652 **Despite limited changes to the GA*TC methylome, *metJ* and *dam* interact to influence *S.***
653 **Typhimurium invasion and motility**
654 Having successfully used Δ*dam* transcriptomics to identify one biologically meaningful
655 co-occurrence of differential expression and methylation, we next attempted to leverage Δ*dam*
656 mutants to test our hypothesis that aberrant methylation in Δ*metJ* bacteria contribute to the impact
657 of Δ*metJ* on invasion and motility (91). Importantly, we observed a small growth defect in Δ*dam*
658 and Δ*dam*Δ*metJ* bacteria, and so all bacteria used for these experiments were grown an extra 30
659 minutes prior to infection to standardize the growth phase used. Knocking out *dam* only modestly
660 reduced the impact of Δ*metJ* on invasion and is therefore unlikely to be the primary mechanism
661 by which *metJ* deletion impacts invasion **(Figure 7A)**. In contrast, impairment in motility caused
662 by *metJ* deletion was completely abrogated in Δ*dam* genetic background, suggesting that *dam* and
663 *metJ* impact motility through the same pathway **(Figure 7B)**. Importantly, comparing isogenic
664 strains (wild-type vs Δ*metJ*; Δ*dam* vs Δ*dam*Δ*metJ;* Δ*dam* p*dam* vs Δ*dam*Δ*metJ* p*dam*) revealed
665 that complementation of *dam* on a low copy number plasmid (pWSK129) restored differences
666 between Δ*dam* and Δ*dam*Δ*metJ* bacteria, though we observed that *dam* complementation itself
667 reduces motility further. This is likely due to modest *dam* overexpression, which has previously
668 been reported to be a more potent inhibitor of *S.* Typhimurium 14028s motility than *dam* deletion
669 (34).
670
671 **The motility defect of Δ*metJ S.* Typhimurium partially depends on *tsr***
672 We hypothesized that the genetic interaction between *dam* and *metJ* could signify that
673 differential GA*TC methylation in the Δ*metJ* mutant suppresses bacterial motility. In striking
674 contrast to this hypothesis, our combined binary dataset revealed no genes that were both
675 differentially GA*TC methylated and expressed (except for the deleted *metJ* itself) **(Table 5)**. We
676 next turned to our percent methylation data to examine whether a shift in methylation could explain
677 differences in flagellar gene regulation between the two bacteria. Comparing percent methylation
678 in both methylation datasets at all GA*TC methylated sites in which the nearest gene is
679 differentially expressed identified 17 sites that had a ≥10% average difference in methylation
680 between wild-type and Δ*metJ* bacteria **(Figure 7C).** Because co-occurrence of differential
681 methylation and differential expression is expected to occur frequently by chance, we sought to
682 limit our analyses to bases most likely to impact gene expression. To do this, we restricted our

search to GA*TC sites that are upstream of differentially expressed genes and found two sites of interest. Specifically, these sites are both strands of a single GATC motif upstream of the chemotaxis gene *tsr* that shows elevated methylation in Δ*metJ* **(Figure 7D and 7E, Table 6).**

This hypermethylation led us to hypothesize that increased methylation upstream of *tsr* in Δ*metJ* could decrease *tsr* expression and thereby reduce motility. In line with this hypothesis, replacing *tsr* with a kanamycin resistance cassette partially ablated the ability for Δ*metJ* to cause a motility defect **(Figure 7F,** interaction term p=0.005**)**. Curiously, a search for the methylation-sensitive transcription factor CRP (41) binding motif (AAATGTGATCTAGATCACATTT) in the *tsr* promoter with the MEME FIMO Tool (99) demonstrated that the hypermethylated residue lies within a putative CRP binding site. Together, these data tentatively support a model in which hypermethylation upstream of *tsr* in Δ*metJ* may contribute to the motility defect. However, additional studies are necessary to confirm a causal relationship.

**Increased Methylation in the *flhDC* promoter does not contribute to the Δ*metJ* motility defect**

Given that unlike Δ*dam* (**Figure 7B),** Δ*tsr* does not account for the entire impact of *metJ* deletion on motility **(Figure 7F**, Ratio of Δ*tsr::kan*Δ*metJ*/Δ*tsr::kan* = 0.9**)**, we hypothesized that there may be additional differences in GA*TC methylation between wild-type and Δ*metJ* bacteria that impact motility. Further examination of our quantitative methylation dataset **(Table 6)** revealed one additional plausible hypothesis: a site in the *flhDC* promoter (-278) that barely missed our 10% threshold (9.5% more methylated in Δ*metJ* bacteria). We decided to test this site as well, as FlhDC make up the master flagellar regulator and thus modest methylated-mediated regulation of the operon could explain our findings. To test whether differential methylation of the *flhDC* promoter could explain the motility defect in Δ*metJ*, we performed site directed mutagenesis on the *S.* Typhimurium chromosome to mutate the base from GATC to GTTC. However, this mutation had no effect on motility in wild-type or Δ*metJ* bacteria **(Supplemental Figure 9)**, disproving the hypothesis that this site could contribute to the Δ*dam* epistatic effect. Notably, this does not rule out that hypermethylation of this site could play a role in flagellar gene expression in other contexts but does demonstrate that it does not contribute to the Δ*metJ* motility defect.

## Discussion

In this work, we demonstrate that at the genome-wide level differential methylation and differential expression are not correlated. Under the critical conditions of SPI-1 or SPI-2 induction, we observed no association between DEGs and DMGs, whether examining binary changes in methylation or quantitative shifts in methylation of >10%. However, our results do demonstrate that genome-wide methylation studies of biologically relevant conditions can be integrated with data from methylase knockout mutants to identify methyl-bases that may be coupled with gene expression, as exemplified by the *stdA* and *tsr* examples. Integration of data from future methylomic studies with our publicly available datasets could reveal additional naturally occurring instances and potentially important co-occurrence of differential methylation and differential expression. As our work demonstrates, such instances will likely be challenging to identify, as they do not occur more often than expected by chance, and therefore do not appear to be a general mechanism of gene regulation in *Salmonella.* Additionally, we hope that this work encourages the generation of additional methylomic datasets under diverse and biologically relevant conditions in order to enable more intra-species comparative methylomics.

A surprising aspect of our work was that the most differentially active methylase we observed, YhdJ, appears to have almost no impact on the *S.* Typhimurium transcriptome under

729 standard conditions. In contrast to Dam which has known impacts on DNA and bacterial
730 replication (10-19), YhdJ also appears to be completely non-essential for *S.* Typhimurium fitness
731 under our growth conditions and in mice. This raises questions about the broader role of DNA
732 methylation, and in particular YhdJ methylation, in the bacterial cell. One tantalizing hypothesis
733 is that YhdJ plays a role in phage defense, which would have been missed studying the conditions
734 here. Alternatively, YhdJ may contribute to physical genomic structural stability under stress
735 conditions, similar to a proposed role for Dam during antibiotic treatment (32). While these
736 hypotheses could explain why YhdJ does not impact gene expression, they fail to address why we
737 observed reproducible changes in the YhdJ methylome across different conditions. As an answer
738 to this, we speculate that these differences are due to changes in the accessibility of YhdJ to
739 ATGCAT motifs under the different conditions, rather than intentional targeting of YhdJ to these
740 sites. This could be due to differences in other genomic modifications that antagonize YhdJ
741 function, altered protein-DNA interactions that mask ATGCAT sites, and/or changes to the 3D
742 conformation of the genome that prevent interactions between YhdJ and its motif.
743 We propose three potential explanations for the lack of a consistent correlation between
744 global $m^6A$ DNA methylation and gene expression in our data. The first is that while *S.*
745 Typhimurium can and do use $m^6A$ methylation as a mechanism to promote bistability or otherwise
746 regulate transcription, they do so sparingly. This would suggest that while the canonical examples
747 of this are elegant (12,21,22,29,30,36,54-58,98), they are rare exceptions to the general rules of *S.*
748 Typhimurium gene regulation. While we are certainly not the first to discover individual sites of
749 differential $m^6A$ methylation that do not correlate with gene expression (100,101), this is the first
750 analysis to demonstrate how widespread the phenomenon is in *S*. Typhimurium. The second
751 hypothesis is that three of the four conditions tested here (wild-type or Δ*metJ* bacteria grown in
752 LB or SPI-2 inducing media) are non-representative conditions, whereas our results with the wild-
753 type vs Δ*metJ* in SPI-2 media are more representative of methylation's relationship with
754 transcription. Notably, while this is possible, these conditions were specifically chosen as they are
755 (a) relevant to the pathogenic capacity of the bacteria, (b) the conditions most frequently studied
756 in laboratory settings, or (c) disrupt metabolic pathways directly connected to methylation.
757 Therefore, even if methylation plays larger roles in regulating gene expression under other
758 conditions (*e.g.* nutrient poor conditions at ambient temperature, following phage insult, etc.), our
759 findings would still suggest that most observed *S.* Typhimurium phenomenon are unlikely to be
760 linked to changes in $m^6A$ methylation. The third possibility is that while $m^6A$ is the most common
761 modification to the *S.* Typhimurium genome, other modifications ($m^5C$, phosphorothioation, *etc*.)
762 may have more important impacts on gene expression.
763 In conclusion, through this work we have increased our understanding of the *S.*
764 Typhimurium methylome by defining it as a highly stable system that is largely decoupled from
765 the transcriptome at the genome-wide level. We hope that this work will serve as a reference for
766 how to perform, analyze, and follow-up on DNA methylation studies, and that it will help redefine
767 how we think about $m^6A$ methylation in bacteria.
768
769 **Data Availability**
770 All sequencing data is available in the NCBI's Gene Expression Omnibus (GEO) (102)
771 Super Series (GSE185077). This includes both SMRT-seq experiments (GSE185578 and
772 GSE185501), as well as both RNA-seq experiments (GSE185072 and GSE185073). All biological
773 resources are available upon request to Dr. Dennis Ko.
774

**Acknowledgements**

The authors would like to thank the Duke University School of Medicine for the use of the Sequencing and Genomic Technologies Shared Resource for performing the library preparations and sequencing experiments referenced throughout this paper. We thank Dr. David Corcoran for supervising the genomic analyses performed by J.L.M and W.C. We thank Kristin Cleveland and Duke DLAR Breeding Core personnel for breeding and maintenance of mouse lines. pREDTKI (Addgene plasmid # 51628 ; http://n2t.net/addgene:51628 ; RRID:Addgene_51628), pMDIAI (Addgene plasmid # 51655 ; http://n2t.net/addgene:51655 ; RRID:Addgene_51655), and pKSI-1(Addgene plasmid # 51725 ; http://n2t.net/addgene:51725 ; RRID:Addgene_51725) were gifts from Sheng Yang. We also thank all past and present members of the Ko lab, especially Kyle Gibbs, Alejandro Antonia, Alyson Barnes, Rachel Keener, Angela Jones, and Margaret Gaggioli for their helpful discussions about the manuscript. Finally, we are grateful to Dr. Stacy Horner and the Duke Molecular Genetics and Microbiology department for use of equipment and shared resources. All schematic images were generated using Biorender.com.

**Funding**

This work was supported by the National Institutes of Health [1F31AI143147 to JSB, R01AI118903 to DCK, R21AI144586 to DCK]. The funders played no role in the study design, data collection and analysis, decision to publish, or preparation of the manuscript.

**Conflict of Interest**

No authors report a conflict of interest.

**References**

1. Frommer, M., McDonald, L.E., Millar, D.S., Collis, C.M., Watt, F., Grigg, G.W., Molloy, P.L. and Paul, C.L. (1992) A genomic sequencing protocol that yields a positive display of 5-methylcytosine residues in individual DNA strands. *Proc Natl Acad Sci U S A*, **89**, 1827-1831.
2. Loenen, W.A., Dryden, D.T., Raleigh, E.A., Wilson, G.G. and Murray, N.E. (2014) Highlights of the DNA cutters: a short history of the restriction enzymes. *Nucleic Acids Res*, **42**, 3-19.
3. Glickman, B.W. and Radman, M. (1980) Escherichia coli mutator mutants deficient in methylation-instructed DNA mismatch correction. *Proc Natl Acad Sci U S A*, **77**, 1063-1067.
4. Pukkila, P.J., Peterson, J., Herman, G., Modrich, P. and Meselson, M. (1983) Effects of high levels of DNA adenine methylation on methyl-directed mismatch repair in Escherichia coli. *Genetics*, **104**, 571-582.
5. Glickman, B.W. (1979) Spontaneous mutagenesis in Escherichia coli strains lacking 6-methyladenine residues in their DNA: an altered mutational spectrum in dam- mutants. *Mutat Res*, **61**, 153-162.
6. Schlagman, S.L., Hattman, S. and Marinus, M.G. (1986) Direct role of the Escherichia coli Dam DNA methyltransferase in methylation-directed mismatch repair. *Journal of bacteriology*, **165**, 896-900.

819 7. Torreblanca, J. and Casadesus, J. (1996) DNA adenine methylase mutants of Salmonella
820 typhimurium and a novel dam-regulated locus. *Genetics*, **144**, 15-26.
821 8. Robinson, V.L., Oyston, P.C. and Titball, R.W. (2005) A dam mutant of Yersinia pestis is
822 attenuated and induces protection against plague. *FEMS Microbiol Lett*, **252**, 251-256.
823 9. Watson, M.E., Jr., Jarisch, J. and Smith, A.L. (2004) Inactivation of deoxyadenosine
824 methyltransferase (dam) attenuates Haemophilus influenzae virulence. *Mol Microbiol*,
825 **53**, 651-664.
826 10. Julio, S.M., Heithoff, D.M., Provenzano, D., Klose, K.E., Sinsheimer, R.L., Low, D.A. and
827 Mahan, M.J. (2001) DNA adenine methylase is essential for viability and plays a role in the
828 pathogenesis of Yersinia pseudotuberculosis and Vibrio cholerae. *Infect Immun*, **69**, 7610-
829 7615.
830 11. Chao, M.C., Zhu, S., Kimura, S., Davis, B.M., Schadt, E.E., Fang, G. and Waldor, M.K. (2015)
831 A Cytosine Methyltransferase Modulates the Cell Envelope Stress Response in the Cholera
832 Pathogen [corrected]. *PLoS Genet*, **11**, e1005666.
833 12. Collier, J., McAdams, H.H. and Shapiro, L. (2007) A DNA methylation ratchet governs
834 progression through a bacterial cell cycle. *Proc Natl Acad Sci U S A*, **104**, 17111-17116.
835 13. Stephens, C., Reisenauer, A., Wright, R. and Shapiro, L. (1996) A cell cycle-regulated
836 bacterial DNA methyltransferase is essential for viability. *Proc Natl Acad Sci U S A*, **93**,
837 1210-1214.
838 14. Zweiger, G., Marczynski, G. and Shapiro, L. (1994) A Caulobacter DNA methyltransferase
839 that functions only in the predivisional cell. *J Mol Biol*, **235**, 472-485.
840 15. Campbell, J.L. and Kleckner, N. (1990) E. coli oriC and the dnaA gene promoter are
841 sequestered from dam methyltransferase following the passage of the chromosomal
842 replication fork. *Cell*, **62**, 967-979.
843 16. Campellone, K.G., Roe, A.J., Lobner-Olesen, A., Murphy, K.C., Magoun, L., Brady, M.J.,
844 Donohue-Rolfe, A., Tzipori, S., Gally, D.L., Leong, J.M. *et al.* (2007) Increased adherence
845 and actin pedestal formation by dam-deficient enterohaemorrhagic Escherichia coli
846 O157:H7. *Mol Microbiol*, **63**, 1468-1481.
847 17. Erova, T.E., Pillai, L., Fadl, A.A., Sha, J., Wang, S., Galindo, C.L. and Chopra, A.K. (2006) DNA
848 adenine methyltransferase influences the virulence of Aeromonas hydrophila. *Infect*
849 *Immun*, **74**, 410-424.
850 18. Mehling, J.S., Lavender, H. and Clegg, S. (2007) A Dam methylation mutant of Klebsiella
851 pneumoniae is partially attenuated. *FEMS Microbiol Lett*, **268**, 187-193.
852 19. Taylor, V.L., Titball, R.W. and Oyston, P.C.F. (2005) Oral immunization with a dam mutant
853 of Yersinia pseudotuberculosis protects against plague. *Microbiology (Reading)*, **151**,
854 1919-1926.
855 20. Henderson, I.R. and Owen, P. (1999) The major phase-variable outer membrane protein
856 of Escherichia coli structurally resembles the immunoglobulin A1 protease class of
857 exported protein and is regulated by a novel mechanism involving Dam and oxyR. *Journal*
858 *of bacteriology*, **181**, 2132-2141.
859 21. Cota, I., Blanc-Potard, A.B. and Casadesus, J. (2012) STM2209-STM2208 (opvAB): a phase
860 variation locus of Salmonella enterica involved in control of O-antigen chain length. *PLoS*
861 *One*, **7**, e36863.

862 22. Broadbent, S.E., Davies, M.R. and van der Woude, M.W. (2010) Phase variation controls
863 expression of Salmonella lipopolysaccharide modification genes by a DNA methylation-
864 dependent mechanism. *Mol Microbiol*, **77**, 337-353.
865 23. Falker, S., Schilling, J., Schmidt, M.A. and Heusipp, G. (2007) Overproduction of DNA
866 adenine methyltransferase alters motility, invasion, and the lipopolysaccharide O-antigen
867 composition of Yersinia enterocolitica. *Infect Immun*, **75**, 4990-4997.
868 24. Sarnacki, S.H., Marolda, C.L., Noto Llana, M., Giacomodonato, M.N., Valvano, M.A. and
869 Cerquetti, M.C. (2009) Dam methylation controls O-antigen chain length in Salmonella
870 enterica serovar enteritidis by regulating the expression of Wzz protein. *Journal of*
871 *bacteriology*, **191**, 6694-6700.
872 25. Sarnacki, S.H., Castaneda Mdel, R., Noto Llana, M., Giacomodonato, M.N., Valvano, M.A.
873 and Cerquetti, M.C. (2013) Dam methylation participates in the regulation of PmrA/PmrB
874 and RcsC/RcsD/RcsB two component regulatory systems in Salmonella enterica serovar
875 Enteritidis. *PLoS One*, **8**, e56474.
876 26. Murphy, K.C., Ritchie, J.M., Waldor, M.K., Lobner-Olesen, A. and Marinus, M.G. (2008)
877 Dam methyltransferase is required for stable lysogeny of the Shiga toxin (Stx2)-encoding
878 bacteriophage 933W of enterohemorrhagic Escherichia coli O157:H7. *Journal of*
879 *bacteriology*, **190**, 438-441.
880 27. Gordeeva, J., Morozova, N., Sierro, N., Isaev, A., Sinkunas, T., Tsvetkova, K., Matlashov,
881 M., Truncaite, L., Morgan, R.D., Ivanov, N.V. *et al.* (2019) BREX system of Escherichia coli
882 distinguishes self from non-self by methylation of a specific DNA site. *Nucleic Acids Res*,
883 **47**, 253-265.
884 28. Torreblanca, J., Marques, S. and Casadesus, J. (1999) Synthesis of FinP RNA by plasmids F
885 and pSLT is regulated by DNA adenine methylation. *Genetics*, **152**, 31-45.
886 29. Camacho, E.M. and Casadesus, J. (2005) Regulation of traJ transcription in the Salmonella
887 virulence plasmid by strand-specific DNA adenine hemimethylation. *Mol Microbiol*, **57**,
888 1700-1718.
889 30. Blyn, L.B., Braaten, B.A. and Low, D.A. (1990) Regulation of pap pilin phase variation by a
890 mechanism involving differential dam methylation states. *EMBO J*, **9**, 4045-4054.
891 31. Balbontin, R., Rowley, G., Pucciarelli, M.G., Lopez-Garrido, J., Wormstone, Y., Lucchini, S.,
892 Garcia-Del Portillo, F., Hinton, J.C. and Casadesus, J. (2006) DNA adenine methylation
893 regulates virulence gene expression in Salmonella enterica serovar Typhimurium. *Journal*
894 *of bacteriology*, **188**, 8160-8168.
895 32. Cohen, N.R., Ross, C.A., Jain, S., Shapiro, R.S., Gutierrez, A., Belenky, P., Li, H. and Collins,
896 J.J. (2016) A role for the bacterial GATC methylome in antibiotic stress survival. *Nat Genet*,
897 **48**, 581-586.
898 33. Shell, S.S., Prestwich, E.G., Baek, S.H., Shah, R.R., Sassetti, C.M., Dedon, P.C. and Fortune,
899 S.M. (2013) DNA methylation impacts gene expression and ensures hypoxic survival of
900 Mycobacterium tuberculosis. *PLoS Pathog*, **9**, e1003419.
901 34. Badie, G., Heithoff, D.M., Sinsheimer, R.L. and Mahan, M.J. (2007) Altered levels of
902 Salmonella DNA adenine methylase are associated with defects in gene expression,
903 motility, flagellar synthesis, and bile resistance in the pathogenic strain 14028 but not in
904 the laboratory strain LT2. *Journal of bacteriology*, **189**, 1556-1564.

905 35. Oliveira, P.H., Ribis, J.W., Garrett, E.M., Trzilova, D., Kim, A., Sekulovic, O., Mead, E.A., Pak,
906 T., Zhu, S., Deikus, G. *et al.* (2020) Epigenomic characterization of Clostridioides difficile
907 finds a conserved DNA methyltransferase that mediates sporulation and pathogenesis.
908 *Nat Microbiol*, **5**, 166-180.
909 36. Brunet, Y.R., Bernard, C.S., Gavioli, M., Lloubes, R. and Cascales, E. (2011) An epigenetic
910 switch involving overlapping fur and DNA methylation optimizes expression of a type VI
911 secretion gene cluster. *PLoS Genet*, **7**, e1002205.
912 37. Chen, L., Paulsen, D.B., Scruggs, D.W., Banes, M.M., Reeks, B.Y. and Lawrence, M.L. (2003)
913 Alteration of DNA adenine methylase (Dam) activity in Pasteurella multocida causes
914 increased spontaneous mutation frequency and attenuation in mice. *Microbiology*
915 *(Reading)*, **149**, 2283-2290.
916 38. Heithoff, D.M., Sinsheimer, R.L., Low, D.A. and Mahan, M.J. (1999) An essential role for
917 DNA adenine methylation in bacterial virulence. *Science*, **284**, 967-970.
918 39. Garcia-Del Portillo, F., Pucciarelli, M.G. and Casadesus, J. (1999) DNA adenine methylase
919 mutants of Salmonella typhimurium show defects in protein secretion, cell invasion, and
920 M cell cytotoxicity. *Proc Natl Acad Sci U S A*, **96**, 11578-11583.
921 40. Atack, J.M., Tan, A., Bakaletz, L.O., Jennings, M.P. and Seib, K.L. (2018) Phasevarions of
922 Bacterial Pathogens: Methylomics Sheds New Light on Old Enemies. *Trends Microbiol*, **26**,
923 715-726.
924 41. Sanchez-Romero, M.A. and Casadesus, J. (2020) The bacterial epigenome. *Nat Rev*
925 *Microbiol*, **18**, 7-20.
926 42. Beaulaurier, J., Schadt, E.E. and Fang, G. (2019) Deciphering bacterial epigenomes using
927 modern sequencing technologies. *Nat Rev Genet*, **20**, 157-172.
928 43. Marinus, M.G. and Lobner-Olesen, A. (2014) DNA Methylation. *EcoSal Plus*, **6**.
929 44. Flusberg, B.A., Webster, D.R., Lee, J.H., Travers, K.J., Olivares, E.C., Clark, T.A., Korlach, J.
930 and Turner, S.W. (2010) Direct detection of DNA methylation during single-molecule, real-
931 time sequencing. *Nature methods*, **7**, 461-465.
932 45. Rand, A.C., Jain, M., Eizenga, J.M., Musselman-Brown, A., Olsen, H.E., Akeson, M. and
933 Paten, B. (2017) Mapping DNA methylation with high-throughput nanopore sequencing.
934 *Nature methods*, **14**, 411-413.
935 46. Tourancheau, A., Mead, E.A., Zhang, X.S. and Fang, G. (2021) Discovering multiple types
936 of DNA methylation from bacteria and microbiome using nanopore sequencing. *Nature*
937 *methods*, **18**, 491-498.
938 47. Roberts, R.J., Vincze, T., Posfai, J. and Macelis, D. (2015) REBASE--a database for DNA
939 restriction and modification: enzymes, genes and genomes. *Nucleic Acids Res*, **43**, D298-
940 299.
941 48. Cota, I., Bunk, B., Sproer, C., Overmann, J., Konig, C. and Casadesus, J. (2016) OxyR-
942 dependent formation of DNA methylation patterns in OpvABOFF and OpvABON cell
943 lineages of Salmonella enterica. *Nucleic Acids Res*, **44**, 3595-3609.
944 49. Erill, I., Puigvert, M., Legrand, L., Guarischi-Sousa, R., Vandecasteele, C., Setubal, J.C.,
945 Genin, S., Guidot, A. and Valls, M. (2017) Comparative Analysis of Ralstonia solanacearum
946 Methylomes. *Front Plant Sci*, **8**, 504.
947 50. Modlin, S.J., Conkle-Gutierrez, D., Kim, C., Mitchell, S.N., Morrissey, C., Weinrick, B.C.,
948 Jacobs, W.R., Ramirez-Busby, S.M., Hoffner, S.E. and Valafar, F. (2020) Drivers and sites of

949 diversity in the DNA adenine methylomes of 93 Mycobacterium tuberculosis complex
950 clinical isolates. *Elife*, **9**.
951 51. Kahramanoglou, C., Prieto, A.I., Khedkar, S., Haase, B., Gupta, A., Benes, V., Fraser, G.M.,
952 Luscombe, N.M. and Seshasayee, A.S. (2012) Genomics of DNA cytosine methylation in
953 Escherichia coli reveals its role in stationary phase transcription. *Nat Commun*, **3**, 886.
954 52. Davis-Richardson, A.G., Russell, J.T., Dias, R., McKinlay, A.J., Canepa, R., Fagen, J.R., Rusoff,
955 K.T., Drew, J.C., Kolaczkowski, B., Emerich, D.W. *et al.* (2016) Integrating DNA Methylation
956 and Gene Expression Data in the Development of the Soybean-Bradyrhizobium N2-Fixing
957 Symbiosis. *Front Microbiol*, **7**, 518.
958 53. Srivastava, A., Murugaiyan, J., Garcia, J.A.L., De Corte, D., Hoetzinger, M., Eravci, M.,
959 Weise, C., Kumar, Y., Roesler, U., Hahn, M.W. *et al.* (2020) Combined Methylome,
960 Transcriptome and Proteome Analyses Document Rapid Acclimatization of a Bacterium
961 to Environmental Changes. *Front Microbiol*, **11**, 544785.
962 54. Peterson, S.N. and Reich, N.O. (2008) Competitive Lrp and Dam assembly at the pap
963 regulatory region: implications for mechanisms of epigenetic regulation. *J Mol Biol*, **383**,
964 92-105.
965 55. Hernday, A., Krabbe, M., Braaten, B. and Low, D. (2002) Self-perpetuating epigenetic pili
966 switches in bacteria. *Proc Natl Acad Sci U S A*, **99 Suppl 4**, 16470-16476.
967 56. Waldron, D.E., Owen, P. and Dorman, C.J. (2002) Competitive interaction of the OxyR
968 DNA-binding protein and the Dam methylase at the antigen 43 gene regulatory region in
969 Escherichia coli. *Mol Microbiol*, **44**, 509-520.
970 57. Wallecha, A., Munster, V., Correnti, J., Chan, T. and van der Woude, M. (2002) Dam- and
971 OxyR-dependent phase variation of agn43: essential elements and evidence for a new
972 role of DNA methylation. *Journal of bacteriology*, **184**, 3338-3347.
973 58. Garcia-Pastor, L., Sanchez-Romero, M.A., Jakomin, M., Puerta-Fernandez, E. and
974 Casadesus, J. (2019) Regulation of bistability in the std fimbrial operon of Salmonella
975 enterica by DNA adenine methylation and transcription factors HdfR, StdE and StdF.
976 *Nucleic Acids Res*, **47**, 7929-7941.
977 59. Coombes, B.K., Brown, N.F., Valdez, Y., Brumell, J.H. and Finlay, B.B. (2004) Expression
978 and secretion of Salmonella pathogenicity island-2 virulence genes in response to
979 acidification exhibit differential requirements of a functional type III secretion apparatus
980 and SsaL. *J Biol Chem*, **279**, 49804-49815.
981 60. Datsenko, K.A. and Wanner, B.L. (2000) One-step inactivation of chromosomal genes in
982 Escherichia coli K-12 using PCR products. *Proc Natl Acad Sci U S A*, **97**, 6640-6645.
983 61. Yang, J., Sun, B., Huang, H., Jiang, Y., Diao, L., Chen, B., Xu, C., Wang, X., Liu, J., Jiang, W.
984 *et al.* (2014) High-efficiency scarless genetic modification in Escherichia coli by using
985 lambda red recombination and I-SceI cleavage. *Appl Environ Microbiol*, **80**, 3826-3834.
986 62. Wang, R.F. and Kushner, S.R. (1991) Construction of versatile low-copy-number vectors
987 for cloning, sequencing and gene expression in Escherichia coli. *Gene*, **100**, 195-199.
988 63. Hwang, S., Martinez, D., Perez, P. and Rinaldi, C. (2011) Effect of surfactant-coated iron
989 oxide nanoparticles on the effluent water quality from a simulated sequencing batch
990 reactor treating domestic wastewater. *Environ Pollut*, **159**, 3411-3415.
991 64. Kersey, P.J., Staines, D.M., Lawson, D., Kulesha, E., Derwent, P., Humphrey, J.C., Hughes,
992 D.S., Keenan, S., Kerhornou, A., Koscielny, G. *et al.* (2012) Ensembl Genomes: an

993 integrative resource for genome-scale data from non-vertebrate species. *Nucleic Acids*
994 *Res*, **40**, D91-97.
995 65. Dobin, A., Davis, C.A., Schlesinger, F., Drenkow, J., Zaleski, C., Jha, S., Batut, P., Chaisson,
996 M. and Gingeras, T.R. (2013) STAR: ultrafast universal RNA-seq aligner. *Bioinformatics*, **29**,
997 15-21.
998 66. Love, M.I., Huber, W. and Anders, S. (2014) Moderated estimation of fold change and
999 dispersion for RNA-seq data with DESeq2. *Genome Biol*, **15**, 550.
1000 67. Huber, W., Carey, V.J., Gentleman, R., Anders, S., Carlson, M., Carvalho, B.S., Bravo, H.C.,
1001 Davis, S., Gatto, L., Girke, T. *et al.* (2015) Orchestrating high-throughput genomic analysis
1002 with Bioconductor. *Nature methods*, **12**, 115-121.
1003 68. Alikhan, N.F., Zhou, Z., Sergeant, M.J. and Achtman, M. (2018) A genomic overview of the
1004 population structure of Salmonella. *PLoS Genet*, **14**, e1007261.
1005 69. Achtman, M., Zhou, Z., Alikhan, N.F., Tyne, W., Parkhill, J., Cormican, M., Chiou, C.S.,
1006 Torpdahl, M., Litrup, E., Prendergast, D.M. *et al.* (2020) Genomic diversity of Salmonella
1007 enterica -The UoWUCC 10K genomes project. *Wellcome Open Res*, **5**, 223.
1008 70. Camacho, C., Coulouris, G., Avagyan, V., Ma, N., Papadopoulos, J., Bealer, K. and Madden,
1009 T.L. (2009) BLAST+: architecture and applications. *BMC Bioinformatics*, **10**, 421.
1010 71. Ashburner, M., Ball, C.A., Blake, J.A., Botstein, D., Butler, H., Cherry, J.M., Davis, A.P.,
1011 Dolinski, K., Dwight, S.S., Eppig, J.T. *et al.* (2000) Gene ontology: tool for the unification of
1012 biology. The Gene Ontology Consortium. *Nat Genet*, **25**, 25-29.
1013 72. Gene Ontology, C. (2021) The Gene Ontology resource: enriching a GOld mine. *Nucleic*
1014 *Acids Res*, **49**, D325-D334.
1015 73. Alvarez, M.I., Glover, L.C., Luo, P., Wang, L., Theusch, E., Oehlers, S.H., Walton, E.M., Tram,
1016 T.T.B., Kuang, Y.L., Rotter, J.I. *et al.* (2017) Human genetic variation in VAC14 regulates
1017 Salmonella invasion and typhoid fever through modulation of cholesterol. *Proc Natl Acad*
1018 *Sci U S A*, **114**, E7746-E7755.
1019 74. Jaslow, S.L., Gibbs, K.D., Fricke, W.F., Wang, L., Pittman, K.J., Mammel, M.K., Thaden, J.T.,
1020 Fowler, V.G., Jr., Hammer, G.E., Elfenbein, J.R. *et al.* (2018) Salmonella Activation of STAT3
1021 Signaling by SarA Effector Promotes Intracellular Replication and Production of IL-10. *Cell*
1022 *Rep*, **23**, 3525-3536.
1023 75. Wang, L., Pittman, K.J., Barker, J.R., Salinas, R.E., Stanaway, I.B., Williams, G.D., Carroll,
1024 R.J., Balmat, T., Ingham, A., Gopalakrishnan, A.M. *et al.* (2018) An Atlas of Genetic
1025 Variation Linking Pathogen-Induced Cellular Traits to Human Disease. *Cell Host Microbe*,
1026 **24**, 308-323 e306.
1027 76. Uzzau, S., Figueroa-Bossi, N., Rubino, S. and Bossi, L. (2001) Epitope tagging of
1028 chromosomal genes in Salmonella. *Proc Natl Acad Sci U S A*, **98**, 15264-15269.
1029 77. Schindelin, J., Arganda-Carreras, I., Frise, E., Kaynig, V., Longair, M., Pietzsch, T., Preibisch,
1030 S., Rueden, C., Saalfeld, S., Schmid, B. *et al.* (2012) Fiji: an open-source platform for
1031 biological-image analysis. *Nature methods*, **9**, 676-682.
1032 78. Galan, J.E. and Curtiss, R., 3rd. (1989) Cloning and molecular characterization of genes
1033 whose products allow Salmonella typhimurium to penetrate tissue culture cells. *Proc Natl*
1034 *Acad Sci U S A*, **86**, 6383-6387.

1035 79. Shea, J.E., Hensel, M., Gleeson, C. and Holden, D.W. (1996) Identification of a virulence
1036 locus encoding a second type III secretion system in Salmonella typhimurium. *Proc Natl*
1037 *Acad Sci U S A*, **93**, 2593-2597.
1038 80. Ochman, H., Soncini, F.C., Solomon, F. and Groisman, E.A. (1996) Identification of a
1039 pathogenicity island required for Salmonella survival in host cells. *Proc Natl Acad Sci U S*
1040 *A*, **93**, 7800-7804.
1041 81. Hondorp, E.R. and Matthews, R.G. (2006) Methionine. *EcoSal Plus*, **2**.
1042 82. Cantoni, G.L. (1953) S-Adenosylmethionine; a new intermediate formed enzymatically
1043 from L-methionine and adenosinetriphosphate. *J Biol Chem*, **204**, 403-416.
1044 83. Bigaud, E. and Corrales, F.J. (2016) Methylthioadenosine (MTA) Regulates Liver Cells
1045 Proteome and Methylproteome: Implications in Liver Biology and Disease. *Mol Cell*
1046 *Proteomics*, **15**, 1498-1510.
1047 84. Pascale, R.M., Simile, M.M., Satta, G., Seddaiu, M.A., Daino, L., Pinna, G., Vinci, M.A.,
1048 Gaspa, L. and Feo, F. (1991) Comparative effects of L-methionine, S-adenosyl-L-
1049 methionine and 5'-methylthioadenosine on the growth of preneoplastic lesions and DNA
1050 methylation in rat liver during the early stages of hepatocarcinogenesis. *Anticancer Res*,
1051 **11**, 1617-1624.
1052 85. Woodcock, D.M., Adams, J.K., Allan, R.G. and Cooper, I.A. (1983) Effect of several
1053 inhibitors of enzymatic DNA methylation on the in vivo methylation of different classes of
1054 DNA sequences in a cultured human cell line. *Nucleic Acids Res*, **11**, 489-499.
1055 86. Yi, P., Melnyk, S., Pogribna, M., Pogribny, I.P., Hine, R.J. and James, S.J. (2000) Increase in
1056 plasma homocysteine associated with parallel increases in plasma S-
1057 adenosylhomocysteine and lymphocyte DNA hypomethylation. *J Biol Chem*, **275**, 29318-
1058 29323.
1059 87. Hoffman, D.R., Cornatzer, W.E. and Duerre, J.A. (1979) Relationship between tissue levels
1060 of S-adenosylmethionine, S-adenylhomocysteine, and transmethylation reactions. *Can J*
1061 *Biochem*, **57**, 56-65.
1062 88. Zappia, V., Zydek-Cwick, R. and Schlenk, F. (1969) The specificity of S-adenosylmethionine
1063 derivatives in methyl transfer reactions. *J Biol Chem*, **244**, 4499-4509.
1064 89. Mull, L., Ebbs, M.L. and Bender, J. (2006) A histone methylation-dependent DNA
1065 methylation pathway is uniquely impaired by deficiency in Arabidopsis S-
1066 adenosylhomocysteine hydrolase. *Genetics*, **174**, 1161-1171.
1067 90. Barber, J.R. and Clarke, S. (1984) Inhibition of protein carboxyl methylation by S-adenosyl-
1068 L-homocysteine in intact erythrocytes. Physiological consequences. *J Biol Chem*, **259**,
1069 7115-7122.
1070 91. Bourgeois, J.S., Zhou, D., Thurston, T.L.M., Gilchrist, J.J. and Ko, D.C. (2018)
1071 Methylthioadenosine Suppresses Salmonella Virulence. *Infect Immun*, **86**.
1072 92. Pirone-Davies, C., Hoffmann, M., Roberts, R.J., Muruvanda, T., Timme, R.E., Strain, E., Luo,
1073 Y., Payne, J., Luong, K., Song, Y. *et al.* (2015) Genome-wide methylation patterns in
1074 Salmonella enterica Subsp. enterica Serovars. *PLoS One*, **10**, e0123639.
1075 93. Broadbent, S.E., Balbontin, R., Casadesus, J., Marinus, M.G. and van der Woude, M. (2007)
1076 YhdJ, a nonessential CcrM-like DNA methyltransferase of Escherichia coli and Salmonella
1077 enterica. *Journal of bacteriology*, **189**, 4325-4327.

1078 94. Sanchez-Romero, M.A., Olivenza, D.R., Gutierrez, G. and Casadesus, J. (2020) Contribution
1079 of DNA adenine methylation to gene expression heterogeneity in Salmonella enterica.
1080 *Nucleic Acids Res*.
1081 95. Bailey, T.L., Johnson, J., Grant, C.E. and Noble, W.S. (2015) The MEME Suite. *Nucleic Acids*
1082 *Res*, **43**, W39-49.
1083 96. Kröger, C., Colgan, A., Srikumar, S., Händler, K., Sivasankaran, S.K., Hammarlöf, D.L.,
1084 Canals, R., Grissom, J.E., Conway, T., Hokamp, K. *et al.* (2013), *Cell Host Microbe*, Vol. 14,
1085 pp. 683-695.
1086 97. Jakomin, M., Chessa, D., Baumler, A.J. and Casadesus, J. (2008) Regulation of the
1087 Salmonella enterica std fimbrial operon by DNA adenine methylation, SeqA, and HdfR. *J*
1088 *Bacteriol*, **190**, 7406-7413.
1089 98. Sanchez-Romero, M.A., Olivenza, D.R., Gutierrez, G. and Casadesus, J. (2020) Contribution
1090 of DNA adenine methylation to gene expression heterogeneity in Salmonella enterica.
1091 *Nucleic Acids Res*, **48**, 11857-11867.
1092 99. Grant, C.E., Bailey, T.L. and Noble, W.S. (2011) FIMO: scanning for occurrences of a given
1093 motif. *Bioinformatics*, **27**, 1017-1018.
1094 100. van der Woude, M., Hale, W.B. and Low, D.A. (1998) Formation of DNA methylation
1095 patterns: nonmethylated GATC sequences in gut and pap operons. *J Bacteriol*, **180**, 5913-
1096 5920.
1097 101. Lewis, E.B., Chen, E. and Culyba, M.J. (2021) DNA cytosine methylation at the lexA
1098 promoter of Escherichia coli is stationary phase specific. *G3 (Bethesda)*.
1099 102. Edgar, R., Domrachev, M. and Lash, A.E. (2002) Gene Expression Omnibus: NCBI gene
1100 expression and hybridization array data repository. *Nucleic Acids Res*, **30**, 207-210.
1101
1102

1103 **Figures and Tables**

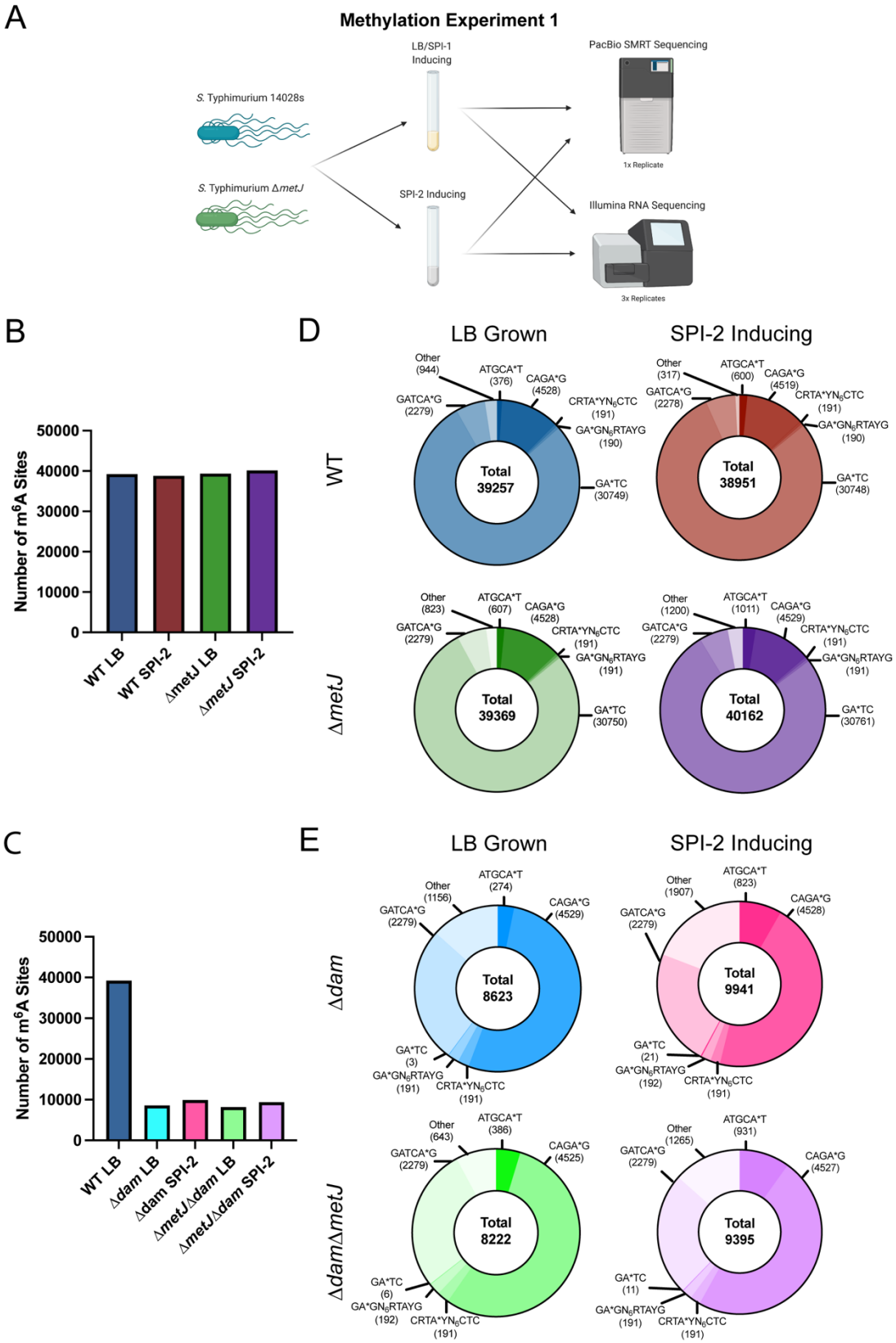


1104

1105 **Figure 1: Genome-wide analysis of $m^6A$ DNA methylation under varying conditions.** (A) Schematic of
1106 Methylation Experiment 1. Wild-type *S.* Typhimurium (Strain 14028s) and an isogenic Δ*metJ* strain were cultured in
1107 LB or *Salmonella* Pathogenicity Island-2 (SPI-2)-inducing media and DNA was collected for SMRT-sequencing.
1108 Bacteria grown under identical conditions were harvested for RNA-sequencing. (B, C) Total number of $m^6A$ bases
1109 observed across conditions does not dramatically change in wild-type and Δ*metJ* bacteria (B), but does change
1110 dramatically in Δ*dam* bacteria (C). (D) Analysis of motifs methylated reveals only the total number of ATGCA*T and
1111 "other" sites (sites that do not map to one of the six motifs) changes dramatically across conditions. (E) Δ*dam* results
1112 in ablation of GATC methylation. For Panels B through E, bases were only included in the analysis if the base could
1113 confidently be called methylated or unmethylated across the eight conditions.

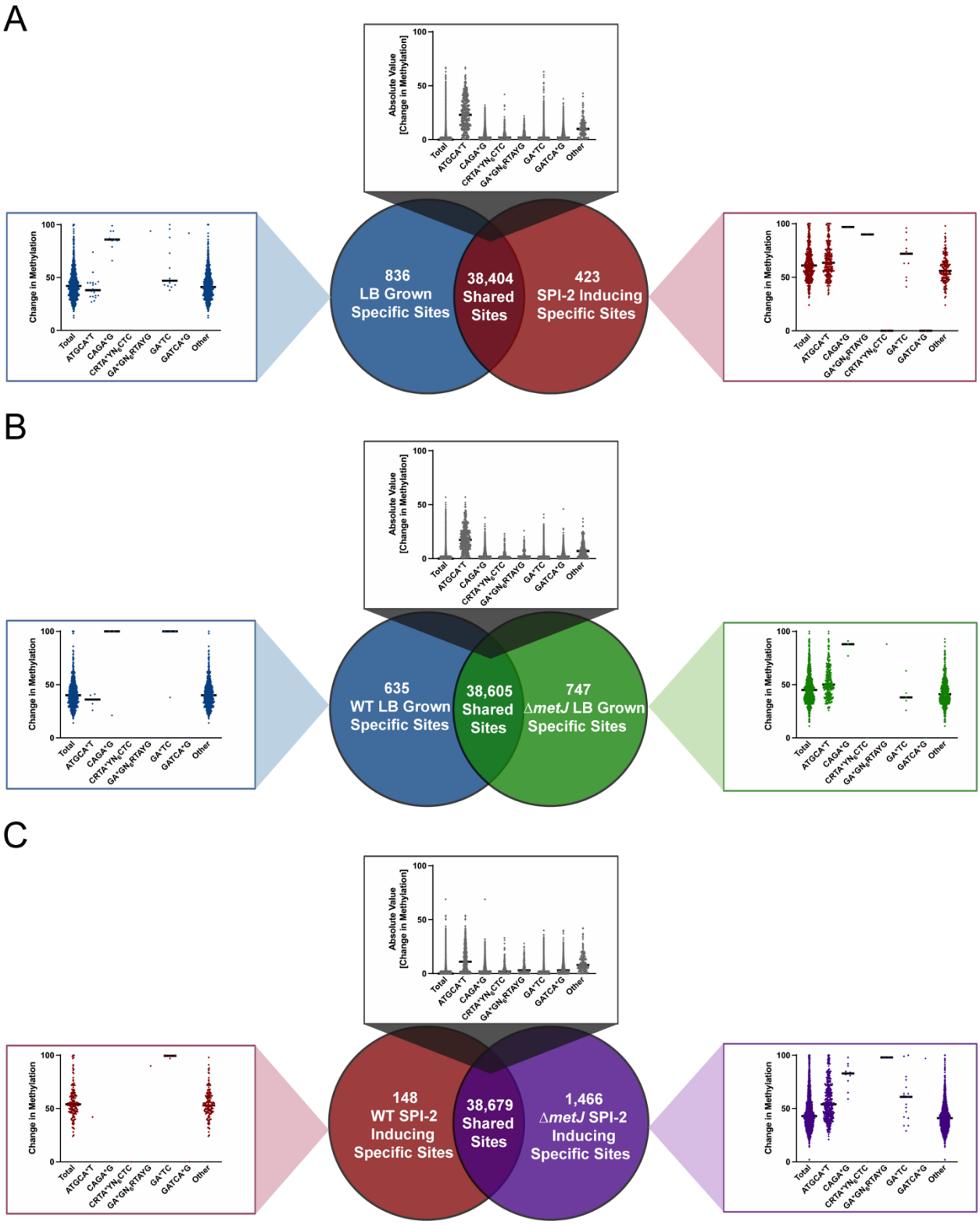


**Figure 2: Integration of binary and quantitative analyses to understand differential methylation in *S. Typhimurium*.** (A-C) Quantification of shared and unique methylated sites between wild-type *S.* Typhimurium grown in LB and SPI-2 inducing media (A), WT and Δ*metJ* bacteria grown in LB (B), and WT and Δ*metJ* bacteria grown in SPI-2 inducing media (C). Venn diagrams are based on binary measures of differential methylation. Sites identified

1120 by the binary analysis were examined in our quantitative dataset in order to identify changes in the percent methylation.
1121 In the graphs "Total" refers to all sites present in the relevant part of the Venn diagram, which were then broken down
1122 by motif. For motifs where no differentially methylated sites were present, a single dot is listed at 0%. For shared
1123 sites, the absolute value of the difference between bases are shown and thus the numbers are agnostic to whether
1124 methylation is higher in either condition. Bars mark the median. For all panels, only bases that could be confidently
1125 called methylated or unmethylated in the eight conditions in **Figure 1** were considered.
1126

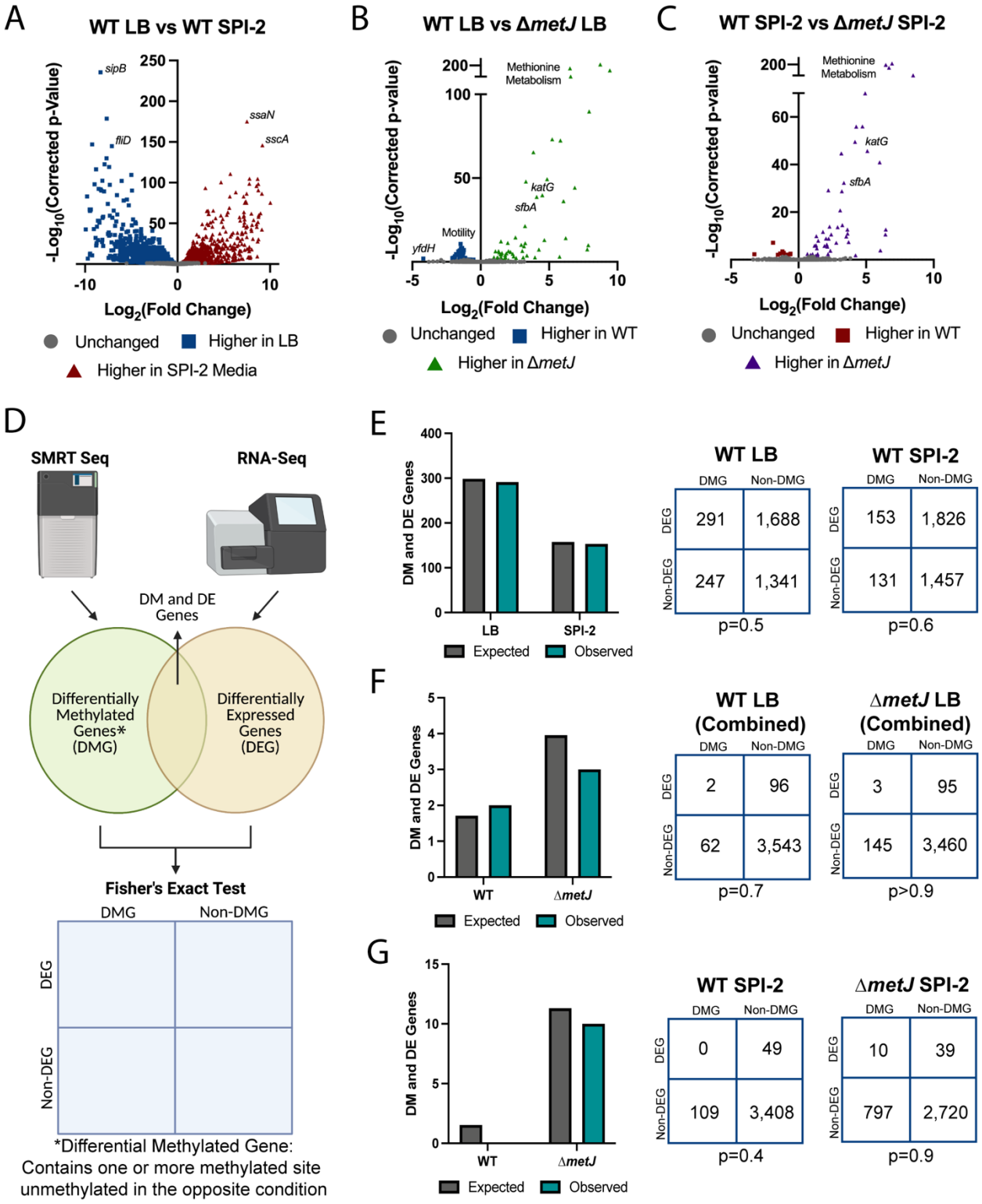


**Figure 3: Differentially methylated genes by binary analysis are not enriched for transcriptomic changes** (A-C) RNA-seq reveals transcriptomic changes between LB grown and SPI-2 media grown wild-type bacteria (A), wild-type and Δ*metJ* bacteria grown in LB (B), and wild-type and Δ*metJ* bacteria grown in SPI-2 media (C). Corrected p-values generated by calculating the false discovery rate. (D) Schematic of RNA-seq and SMRT-seq integration. Each gene was determined to be differentially methylated (Differentially Methylated Gene, DMG) in our binary analysis,

differentially expressed (Differentially Expressed Gene, DEG (FDR<0.05)), differentially methylated and differentially expressed (DM and DE Gene), or neither differentially methylated nor expressed. Fisher's Exact Test was then used to determine whether there was an association between methylation and gene expression. (E-G) Differential methylation is not associated with differential expression. Observed and expected numbers of differentially methylated and differentially expressed genes were not significantly different when comparing uniquely methylated genes in LB vs SPI-2 media (E), wild-type vs Δ*metJ* in LB (F), or wild-type vs Δ*metJ* in SPI-2 media (G). Uniquely methylated genes are plotted in the condition under which they are methylated (*e.g.* for panel E, a gene that contains a base that is methylated in LB but not SPI-2 media would be plotted as part of "LB"), but are agnostic to the direction of effect for the expression data. Expected values are calculated by multiplying the frequency of differential methylation by the frequency of differential expression by the total number of genes in the analysis for each condition. Numbers used for Fisher's Exact Test are shown on the right. Data for E and G used data from Methylation Experiment 1, F used the "Combined Dataset." For F and G the gene *metJ* is removed from the analysis, as it is artificially called both differentially methylated and expressed due to its excision from the genome.

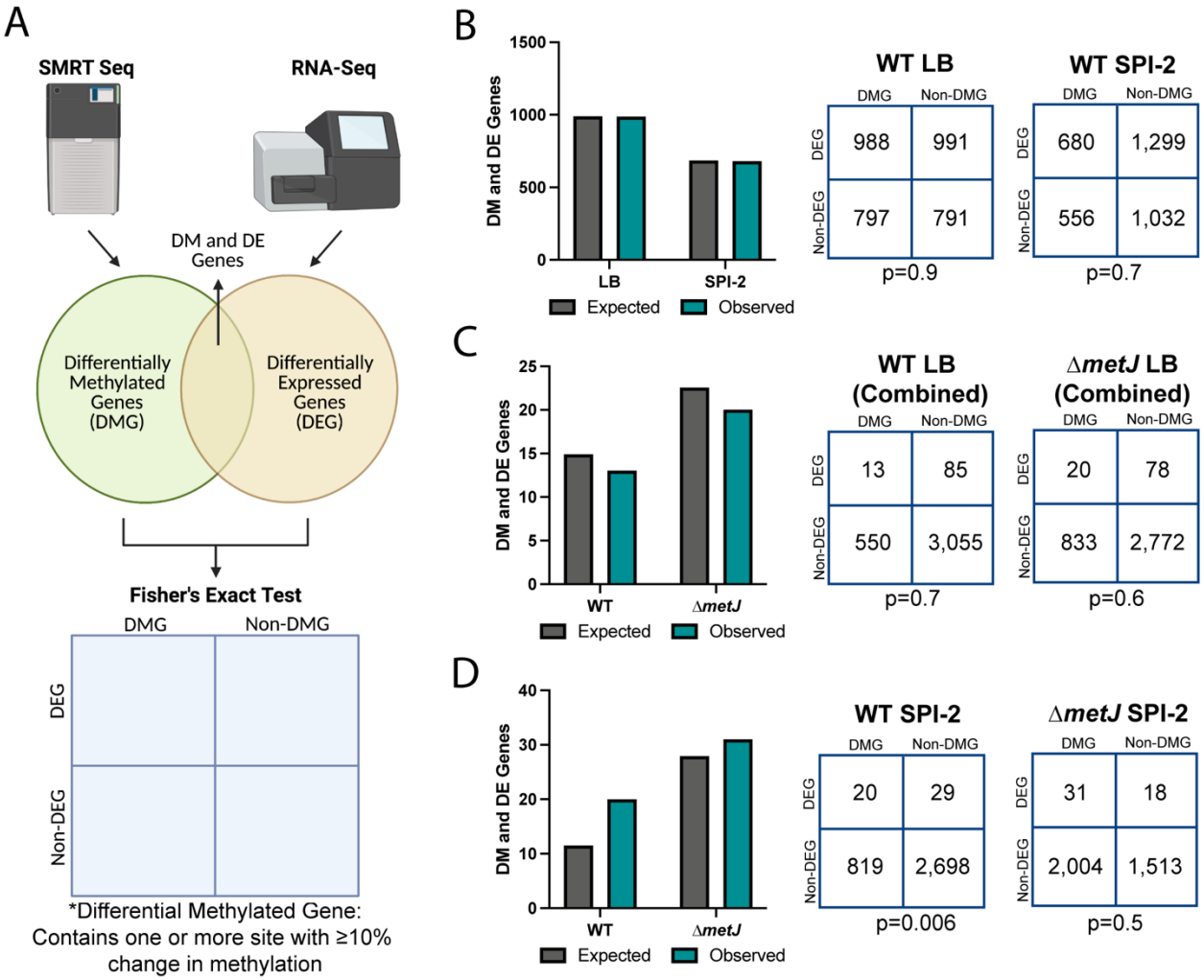


**Figure 4: Quantitative analysis revealed an association between differential methylation and expression between wild-type and Δ*metJ* bacteria.** (A) Schematic of RNA-seq and SMRT-seq integration. Each gene in our quantitative analysis was determined to be differentially methylated (Differentially Methylated Gene, DMG: difference ≥10% methylation across conditions), differentially expressed (Differentially Expressed Gene, DEG: FDR corrected p-value ≤0.05), differentially methylated and differentially expressed (DM and DE Gene), or neither differentially methylated nor expressed. Fisher's Exact Test was then used to determine whether there was an association between methylation and gene expression. (B-D) Differential methylation is typically not associated with differential expression. Observed and expected numbers of differentially methylated and differentially expressed genes were not significantly different when comparing uniquely methylated genes in LB vs SPI-2 media (B), wild-type vs Δ*metJ* in LB (C), however, a significant enrichment of DEGs was observed in hypermethylated sites in wild-type bacteria grown in SPI-2 media relative to Δ*metJ* (D). Hypermethylated genes are plotted in the condition under which they have increased methylation (*e.g.* for panel B, a gene that contains a base that is more methylated in LB would be plotted as part of "LB"), but are agnostic to the direction of effect for the expression data. Expected values are calculated by multiplying the frequency of differential methylation by the frequency of differential expression by the total number of genes in the analysis for each condition. Numbers used for Fisher's Exact Test are shown on the right. Data for B and D used data from Methylation Experiment 1, C used the "Combined Dataset." For C and D the gene *metJ* is removed from the analysis, as it is excised from the genome.

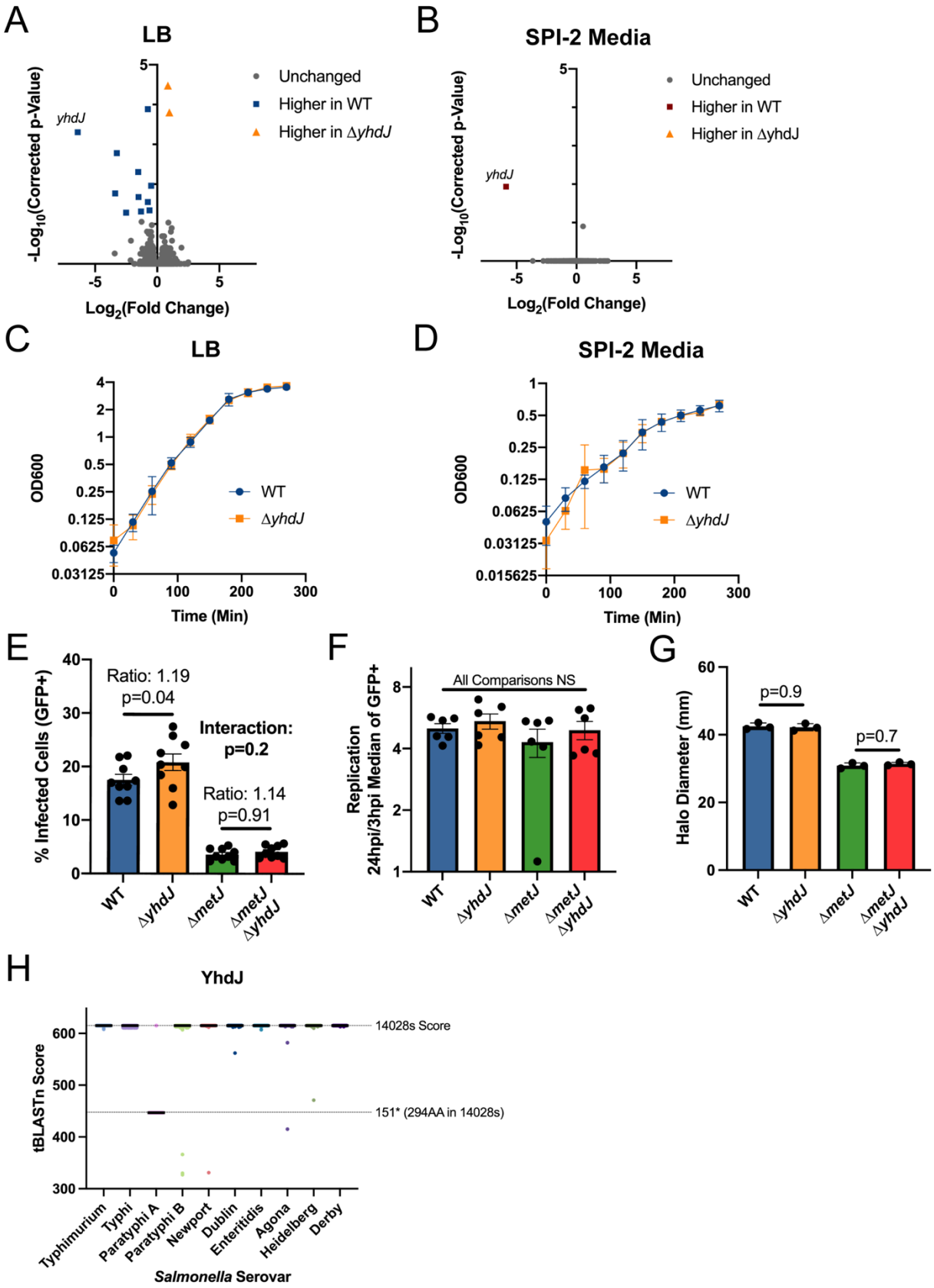
A
LB
Unchanged
Higher in WT
Higher in ΔyhdJ
yhdJ
-Log10(Corrected p-Value)
Log2(Fold Change)
B
SPI-2 Media
Unchanged
Higher in WT
Higher in ΔyhdJ
yhdJ
-Log10(Corrected p-Value)
Log2(Fold Change)
C
LB
OD600
Time (Min)
WT
ΔyhdJ
D
SPI-2 Media
OD600
Time (Min)
WT
ΔyhdJ
E
% Infected Cells (GFP+)
Ratio: 1.19
p=0.04
Interaction:
p=0.2
Ratio: 1.14
p=0.91
WT
ΔyhdJ
ΔmetJ
ΔmetJ ΔyhdJ
F
Replication 24hpi/3hpi Median of GFP+
All Comparisons NS
WT
ΔyhdJ
ΔmetJ
ΔmetJ ΔyhdJ
G
Halo Diameter (mm)
p=0.9
p=0.7
WT
ΔyhdJ
ΔmetJ
ΔmetJ ΔyhdJ
H
YhdJ
tBLASTn Score
14028s Score
151* (294AA in 14028s)
Typhimurium
Typhi
Paratyphi A
Paratyphi B
Newport
Dublin
Enteritidis
Agona
Heidelberg
Derby
Salmonella Serovar

1169

1170 **Figure 5: YhdJ has limited impacts on *S.* Typhimurium biology under standard laboratory conditions.** (A, B).
1171 YhdJ has limited impacts on the *S.* Typhimurium transcriptome in LB (A) and SPI-2 inducing media (B). Corrected
1172 p-values generated by calculating the false discovery rate. (C, D) YhdJ is not required for *S.* Typhimurium growth in
1173 LB (C) or SPI-2 inducing media (D). Data from three independent experiments with time points taken every 30
1174 minutes. Error bars represent the standard error of the mean. (E, F) YhdJ is not required for *S.* Typhimurium uptake
1175 (E) or replication (F) in THP-1 monocytes. Cells were infected for 60 minutes with *S.* Typhimurium harboring an
1176 inducible-GFP plasmid before treatment with gentamicin. GFP was induced for 75 minutes before analysis by flow
1177 cytometry. Percent GFP+ and median of the GFP+ cells were measured three hours and twenty-four hours post
1178 infection. Panel E shows the amount of invasion that occurred by reporting the percent of infected cells at 3 hours post
1179 infection, and Panel F shows the replication that occurred following infection by dividing the median of the GFP+
1180 cells at 24 hours post infection by the median of the GFP+ cells at 3 hours post infection. Data from 2-3 independent
1181 experiments, each dot represents an independent replicate, bars mark the mean, and error bars are the standard error
1182 of the mean. For Panel E, data were normalized to the grand mean before plotting or performing statistics, and for
1183 Panel F statistics were performed on the log transformed values. P-values generated by two-way ANOVA with Sidak's
1184 multiple comparisons test. (G) YhdJ does not impact *S.* Typhimurium motility. Motility on soft agar was measured
1185 six hours after inoculating the agar and following migration at 37°C. Data are from three independent experiments
1186 and each dot is the average of 4-5 technical replicates, bars mark the mean, and error bars mark the standard error of
1187 the mean. Data were normalized to the grand mean prior to plotting or performing statistics. P-values generated by
1188 one-way ANOVA with Sidak's multiple comparisons test. (H) YhdJ is conserved across several *Salmonella* serovars.
1189 *Salmonella* genomes (1,000 Typhimurium, 1,000 Typhi, 1,000 Paratyphi A, 1,000 Paratyphi B, 999 Newport, 1,000
1190 Dublin, 1,000 Enteritidis, 1,000 Agona, 1,000 Heidelberg, and 79 Derby genomes) were obtained from EnteroBase
1191 (68,69). Genomes were combined into a single FASTA file per serovar and blasted against the *S.* Typhimurium strain
1192 14028s YhdJ protein sequence using BLAST+ (70). The BLAST score from the top 'n' hits were plotted, where 'n'
1193 is the number of genomes analyzed for that serovar. Black bar represents the median. Dotted lines represent the
1194 BLAST score obtained when blasting the 14028s genome, and the score obtained from the 151* truncation prevalent
1195 in *S.* Paratyphi A serovars.
1196
1197
1198

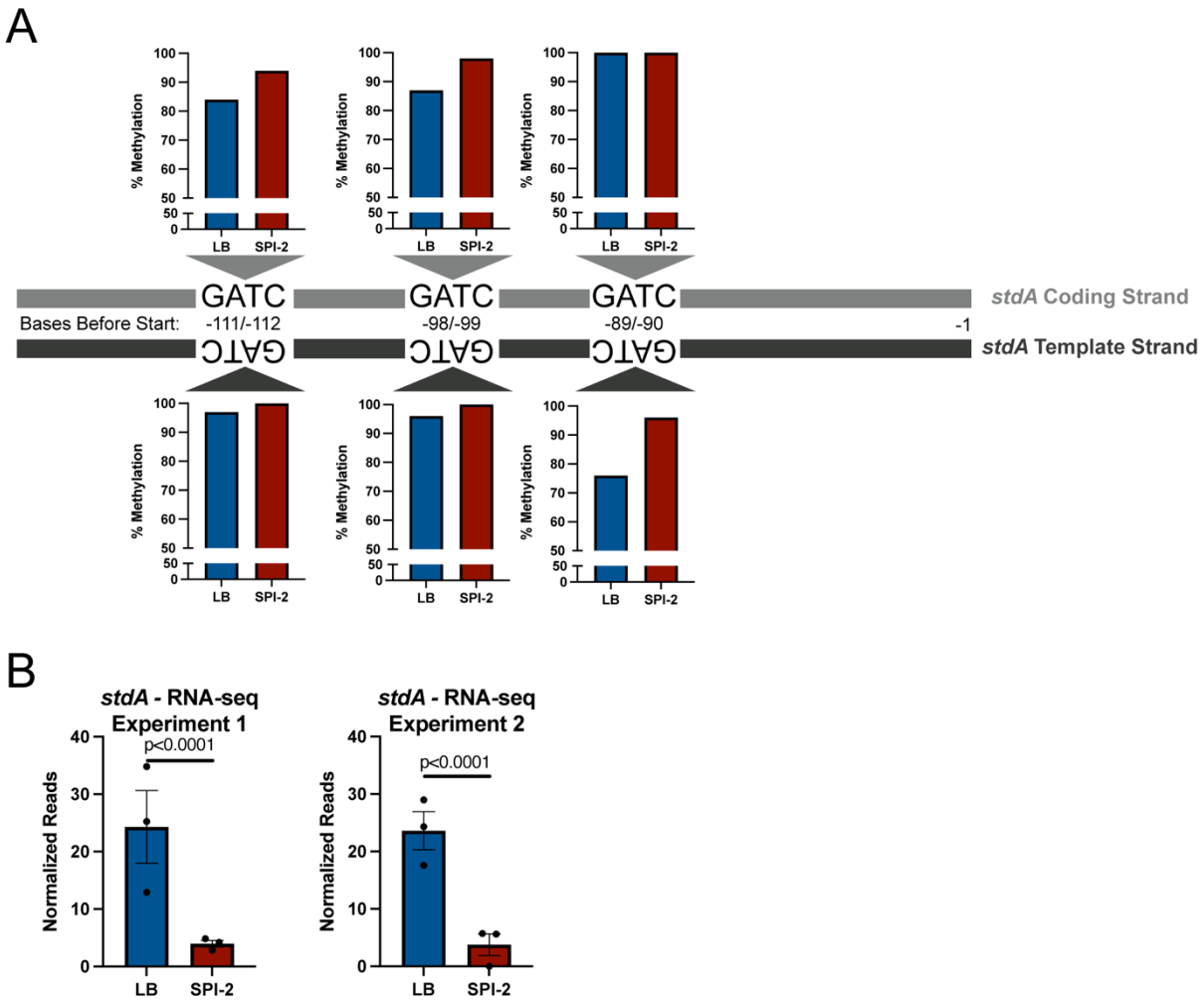


**Figure 6: The *stdA* promoter has differential methylation following growth in LB or SPI-2 inducing media.** (A) Schematic of the region upstream of *stdA*. Percent methylation values for each GATC site on both strands are graphed based on data from wild-type bacteria in Methylation Experiment 1. (B) *stdA* is differentially expressed in wild-type bacteria grown in LB and SPI-2 inducing media. RNA-seq Experiment 1 values are from the RNA-seq experiment including Δ*metJ* and are listed in **Supplemental File 4**. RNA-seq Experiment 2 values are from the experiment including Δ*yhdJ* and are listed in **Supplemental File 5**.

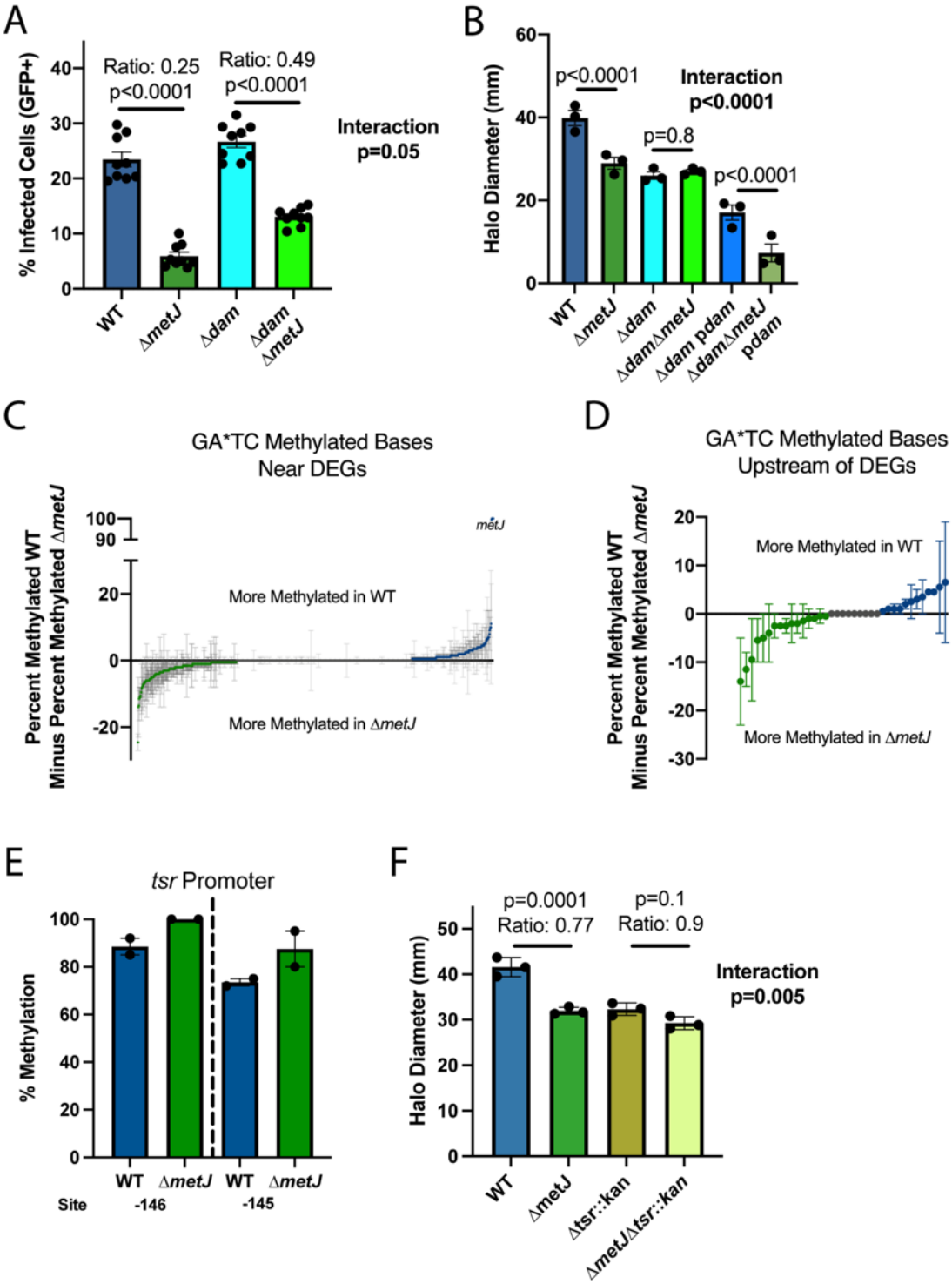


**Figure 7: *dam* is epistatic to Δ*metJ* despite limited changes to the Δ*metJ* GA*TC methylome.** (A) The impacts of Δ*metJ* on invasion partially depend on *dam*. THP-1 monocytes were infected for 60 minutes with *S.* Typhimurium harboring an inducible-GFP plasmid before treatment with gentamicin. GFP was induced for 75 minutes before analysis by flow cytometry. Percent GFP+ was measured three hours post infection. Data are from three experiments, each dot represents an independent replicate, the bars mark the mean, and the error bars are the standard error of the mean. (B) The impact of Δ*metJ* on motility depends entirely on *dam*. Motility on soft agar was measured six hours after inoculating the agar and following migration at 37°C. Data are from three independent experiments and each dot is the mean of 4-5 technical replicates, bars mark the mean, and error bars mark the standard error of the mean. (C,D)

1216 Quantitative analysis reveals subtle changes to the GA*TC methylome in Δ*metJ* bacteria. Each dot represents the
1217 difference average percent methylation of GA*TC bases in which the closest gene in differentially expressed (C), or
1218 GA*TC bases specifically upstream of differentially expressed genes (D), between WT and Δ*metJ* bacteria grown in
1219 LB. Data are in duplicate from the Methylation Experiment 1 and the Replication Methylation Experiment, with error
1220 bars showing the error of the mean. Data from Panel D are expanded in **Table 4.** For C and D, any base with greater
1221 than or less than 0 differential methylation is colored in green (more methylated in Δ*metJ*) or blue (more methylated
1222 in wild-type bacteria). (E) The *tsr* promoter is modestly hypermethylated in Δ*metJ.* Percent methylation is plotted for
1223 the -146 and -145 GATC motifs from the Methylation Experiment 1 and the Replication Methylation Experiment,
1224 with error bars showing the error of the mean. Site numbering is relative to the start codon. (F) The impacts of Δ*metJ*
1225 on motility are partially *tsr* dependent. Data are from three independent experiments and each dot is the mean of 4-5
1226 technical replicates, bars mark the mean, and error bars mark the standard error of the mean. For panels A, B, and F
1227 data were normalized to the grand mean prior to plotting or performing statistics and p-values were generated by two-
1228 way ANOVA with Sidak's multiple comparisons test.

**Table 1: Correlation of differential methylation and differential expression in wild-type *S.* Typhimurium grown in SPI-2 inducing media compared to Δ*metJ* bacteria**

| Genomic Location | WT (SPI-2) % Methylated | Δ*metJ* (SPI-2) % Methylated | Δ %Methylation (WT-Δ*metJ*) | STM14_ID | Common Name | Relative Location | Motif | $log_2$FoldChange (ΔmetJ_SPI-2 / WT_SPI-2) |
|---|---|---|---|---|---|---|---|---|
| NC_016856.1__1217 | 99 | 88 | 11 | STM14_0002 | thrA | Genic | GATCA*G | -1.35 |
| NC_016856.1__277289 | 99 | 88 | 11 | STM14_0276 | ldcC | Genic | GA*TC | 0.89 |
| NC_016856.1__288405 | 98 | 87 | 11 | STM14_0289 | metN | Genic | GA*TC | 4.27 |
| NC_016856.1__572813 | 93 | 74 | 19 | STM14_0601 | sfbB | Genic | CAGA*G | 3.25 |
| NC_016856.1__573231 | 100 | 90 | 10 | STM14_0601 | sfbB | Genic | GA*TC | 3.25 |
| NC_016856.1__573265 | 100 | 81 | 19 | STM14_0601 | sfbB | Genic | GA*TC | 3.25 |
| NC_016856.1__573302 | 100 | 88 | 12 | STM14_0601 | sfbB | Genic | GA*TC | 3.25 |
| NC_016856.1__573803 | 100 | 90 | 10 | STM14_0602 | NA | Genic | GA*TC | 3.62 |
| NC_016856.1__861113 | 100 | 87 | 13 | STM14_0920 | bioB | Genic | GA*TC | -1.22 |
| NC_016856.1__861413 | 100 | 88 | 12 | STM14_0920 | bioB | Genic | GA*TC | -1.22 |
| NC_016856.1__1048140 | 98 | 88 | 10 | STM14_1130 | ompF | Genic | GA*TC | 1.32 |
| NC_016856.1__1423354 | 100 | 89 | 11 | STM14_1619 | thrS | Genic | GA*TC | -0.59 |
| NC_016856.1__1733156 | 76 | 40 | 36 | STM14_1975 | NA | Upstream | Other | 1.46 |
| NC_016856.1__1829331 | 99 | 86 | 13 | STM14_2086 | NA | Genic | GA*TC | 3.63 |
| NC_016856.1__1831286 | 100 | 71 | 29 | STM14_2087 | trpD | Genic | GA*TC | 3.71 |
| NC_016856.1__1834122 | 100 | 84 | 16 | STM14_2089 | trpB | Genic | CAGA*G | 2.13 |
| NC_016856.1__2340851 | 98 | 81 | 17 | STM14_2702 | NA | Genic | GA*TC | 2.79 |
| NC_016856.1__2746393 | 100 | 88 | 12 | STM14_3133 | NA | Genic | GATCA*G | 1.80 |
| NC_016856.1__3270917 | 100 | 88 | 12 | STM14_3733 | metK | Genic | GA*TC | 3.21 |
| NC_016856.1__3272719 | 100 | 88 | 12 | STM14_3735 | NA | Genic | GA*TC | -0.82 |
| NC_016856.1__3722412 | 100 | 90 | 10 | STM14_4260 | asd | Genic | CAGA*G | 2.03 |
| NC_016856.1__4334354 | 100 | 87 | 13 | STM14_4936 | katG | Genic | GA*TC | 5.10 |
| NC_016856.1__4417534 | 100 | 90 | 10 | STM14_5030 | aceA | Genic | GA*TC | 2.42 |
| NC_016856.1__4417670 | 100 | 78 | 22 | STM14_5030 | aceA | Genic | GA*TC | 2.42 |
| NC_016856.1__4423175 | 100 | 89 | 11 | STM14_5035 | metH | Genic | GA*TC | 3.09 |

| | | | | | | | | |
|---|---|---|---|---|---|---|---|---|
| NC_016856.1__4424372 | 100 | 89 | 11 | STM14_5035 | metH | Genic | GA*TC | 3.09 |

*The *metJ* gene is excluded from these analyses due to artificial excision from the genome

1229
1230

**Table 2: Δ*yhdJ* Differential Gene Expression in LB**

| Gene ID | Gene Name | $Log_2$Fold Change (Δ*yhdJ*/WT) | Corrected p-value | ATGCAT Motif? (Relative Location) | Methylated? |
|---|---|---|---|---|---|
| STM14_4375 | *dppA* | -0.75 | 2.95E-08 | **Yes (Genic)** | **Yes** |
| STM14_4084 | *yhdJ* | -6.39 | 2.25E-07 | No | No |
| STM14_5353 | *pyrB* | -3.25 | 1.12E-06 | **Yes (Genic)** | No |
| STM14_4024 | *codB* | -1.52 | 4.51E-06 | No | No |
| STM14_0699 | *cstA* | -0.48 | 1.25E-05 | No | No |
| STM14_5352 | *pyrI* | -3.38 | 2.32E-05 | No | No |
| STM14_0819 | *NA* | 0.85 | 3.34E-05 | No | No |
| STM14_4495 | *pyrE* | -1.49 | 3.84E-05 | No | No |
| STM14_5141 | *acs* | -0.74 | 5.74E-05 | No | No |
| STM14_1558 | *yeaG* | -0.62 | 0.0001 | No | No |
| STM14_3061 | *uraA* | -1.3 | 0.0001 | No | No |
| STM14_0078 | *carB* | -2.49 | 0.0001 | No | No |
| STM14_1885 | *hdeB* | 0.99 | 0.0002 | No | No |

1231
1232
1233
1234
1235
1236
1237
1238
1239
1240

**Table 3: YhdJ does not enhance *S.* Typhimurium fitness in C57BL/6J mice**

| **IP Infection (CFUs from Spleen)** | **Δ*metJ*/WT** | **Δ*yhdJ*/WT** | **Δ*metJ*Δ*yhdJ*/WT** | **Δ*metJ*Δ*yhdJ*/Δ*metJ*** |
|---|---|---|---|---|
| *Number of Mice*[$] | 6 | 8 | 7 | 7 |
| *Median*[#] *(95% Confidence Interval)* | **0.23** (0.07-0.47) | **1.31** (0.60-1.84) | **0.26** (0.13-0.78) | **1.09** (0.000065-2.19) |
| *p-value** | **0.002** | 0.3 | **0.002** | 0.2 |
| **Oral Infection (CFUs from Spleen and Ileum)** | **Δ*yhdJ*/WT (Spleen)** | **Δ*yhdJ*/WT (Ileum)** | | |
| *Number of Mice*[$] | 22 | 21 | | |
| *Median*[#] *(95% Confidence Interval)* | **1.65** (0.72-2.22) | **1.154** (0.74-1.55) | | |
| *p-value** | **0.02** | 0.4 | | |

[$]All mice are age and sex matched, both sexes represented in all experiments, and all data are from at least two experiments
[#]Median competitive index value calculated by dividing the number colonies obtained of each genotype at four days post infection. Median > 1 = numerator strain outcompeted denominator.
*One-sample t-test on log transformed data

1241
1242
1243
1244
1245
1246
1247
1248
1249
1250

**Table 4: Percent methylation of GATC sites in Experiment 1 within 500bp upstream of Δ*dam* differentially expressed virulence genes (based on (31))**

| Gene/Operon (non-listed genes in parentheses) | Base ID | % Methylated in Wild-Type LB | % Methylated in Wild-Type SPI-2 | % Methylated in Δ*dam* LB | % Methylated in Δ*dam* SPI-2 |
|---|---|---|---|---|---|
| *fliC* | 2060552 | 100 | 100 | 0 | 0 |
| | 2060553 | 100 | 88 | 0 | 0 |
| | 2060668 | 100 | 100 | 0 | 0 |
| | 2060669 | 100 | 100 | 0 | 0 |
| | 2060836 | 100 | 100 | 0 | 0 |
| | 2060837 | 100 | 100 | 0 | 0 |
| *fliD (fliS/fliT also in operon)* | 2060552 | 100 | 100 | 0 | 0 |
| | 2060553 | 100 | 88 | 0 | 0 |
| | 2060668 | 100 | 100 | 0 | 0 |
| | 2060669 | 100 | 100 | 0 | 0 |
| *lppB* | 1469508 | 100 | 100 | 0 | 0 |
| | 1469509 | 93 | 100 | 0 | 0 |
| | 1469697 | 100 | 100 | 0 | 0 |
| | 1469698 | 87 | 80 | 0 | 0 |
| *prgH/prgI/prgJ (prg K also in operon)* | None | None | None | None | None |
| *sicA/sipB/sipC* | 3051884 | 92 | 86 | 0 | 0 |
| | 3051885 | 98 | 99 | 0 | 0 |
| | 3051936 | 100 | 100 | 0 | 0 |
| | 3051937 | 100 | 100 | 0 | 0 |
| | 3052008 | 100 | 98 | 0 | 0 |
| | 3052009 | 99 | 100 | 0 | 0 |
| | 3052050 | 100 | 100 | 0 | 0 |
| | 3052051 | 100 | 100 | 0 | 0 |

| | | | | | |
|---|---|---|---|---|---|
| *sipD (sipA/iacP also in operon)* | 3048346 | 100 | 100 | 0 | 0 |
| | 3048347 | 99 | 99 | 0 | 0 |
| *(sopB also in operon) pipC* | 1138389 | 99 | 90 | 0 | 0 |
| | 1138390 | 96 | 97 | 0 | 0 |
| | 1138429 | 99 | 99 | 0 | 0 |
| | 1138430 | 100 | 100 | 0 | 0 |
| | 1138441 | 99 | 100 | 0 | 0 |
| | 1138442 | 100 | 100 | 0 | 0 |
| | 1138525 | 96 | 100 | 0 | 0 |
| | 1138526 | 98 | 100 | 0 | 0 |
| *cheR (STM14_2332/STM14_2331/cheZ also in operon)* | 2026159 | 90 | 99 | 0 | 0 |
| | 2026160 | 96 | 100 | 0 | 0 |
| | 2026385 | 100 | 100 | 0 | 0 |
| | 2026386 | 100 | 100 | 0 | 0 |
| | 2026415 | 100 | 100 | 0 | 0 |
| | 2026416 | 92 | 100 | 0 | 0 |
| *stdA* | 3211770 | 76 | 96 | 0 | 0 |
| | 3211771 | 100 | 100 | 0 | 0 |
| | 3211779 | 96 | 100 | 0 | 0 |
| | 3211780 | 87 | 98 | 0 | 0 |
| | 3211792 | 97 | 100 | 0 | 0 |
| | 3211793 | 84 | 94 | 0 | 0 |
| *stdB/stdC (STM14_3655 also in operon)* | 3210924 | 100 | 100 | 0 | 0 |
| | 3210925 | 100 | 100 | 0 | 0 |
| | 3211283 | 99 | 99 | 0 | 0 |
| | 3211284 | 89 | 95 | 0 | 0 |
| *STM14_3654/STM14_3653* | 3206809 | 100 | 94 | 0 | 0 |

| | | | | | |
|---|---|---|---|---|---|
| | 3206810 | 100 | 100 | 0 | 0 |

| **Table 5: Unique GA*TC sites between wild-type and Δ*metJ S.* Typhimurium (Combined Dataset)** | | | | | |
|---|---|---|---|---|---|
| **Unique WT LB GA*TC Sites** | | | | | |
| *Genomic Location* | *Base* | *Genic Location* | *Gene* | *Product* | *Differentially Expressed?* |
| None | None | None | None | None | N/A |
| | | | | | |
| **Unique Δ*metJ* LB GA*TC Sites** | | | | | |
| *Genomic Location* | *Base* | *Genic Location* | *Gene* | *Product* | *Differentially Expressed?* |
| NC_016856.1 | 1177765 | Upstream | STM14_1293 | N-acetylneuraminate Epimerase | No |
| NC_016856.1 | 4289018 | Downstream | STM14_4888 | CDP-diacylglycerol Pyrophosphatase | No |
| *The *metJ* gene is excluded from these analyses due to artificial excision from the genome | | | | | |

1251
1252
1253
1254
1255
1256
1257
1258
1259
1260
1261
1262
1263
1264

**Table 6: Percent methylation differences for GA*TC motifs upstream of Δ*metJ* differentially expressed genes following growth in LB**

| Base | Closest Gene (STM14 Number) | Closest Gene (Common Name) | % Methylation (WT-Δ*metJ*) Methylation Experiment 1 | % Methylation (WT-Δ*metJ*) Replication Experiment | % Methylation (WT-Δ*metJ*) Average | Gene Expression - $Log_2$Fold Change (Δ*metJ*/WT) | Gene Expression - Corrected p-value |
|---|---|---|---|---|---|---|---|
| 4802770 | STM14_5446 | *tsr* | -23 | -5 | **-14** | -1.28 | 0.006 |
| 4802769 | STM14_5446 | *tsr* | -15 | -8 | **-11.5** | -1.28 | 0.006 |
| 2033749 | STM14_2341 | *flhD* | -1 | -18 | **-9.5** | -0.53 | 0.05 |
| 3243659 | STM14_3699 | *serA* | -10 | -1 | **-5.5** | 1.48 | 5.09E-13 |
| 4415526 | STM14_5029 | *aceB* | -10 | 0 | **-5** | 1.88 | 6.67E-06 |
| 3335887 | STM14_3821 | | 2 | -10 | **-4** | -1.21 | 0.04 |
| 3400695 | STM14_3893 | | 0 | -5 | **-2.5** | -1.32 | 0.007 |
| 3400696 | STM14_3893 | | -2 | -3 | **-2.5** | -1.32 | 0.007 |
| 4415527 | STM14_5029 | *aceB* | -1 | -4 | **-2.5** | 1.88 | 6.67E-06 |
| 2060553 | STM14_2378 | | 2 | -6 | **-2** | -1.52 | 0.0005 |
| 3335886 | STM14_3821 | | -4 | 0 | **-2** | -1.21 | 0.04 |
| 571705 | STM14_0600 | | 2 | -5 | **-1.5** | 4.1 | 1.63E-39 |
| 4415556 | STM14_5029 | *aceB* | -3 | 1 | **-1** | 1.88 | 6.67E-06 |
| 4802790 | STM14_5446 | *tsr* | -1 | -1 | **-1** | -1.28 | 0.006 |
| 3758504 | STM14_4305 | | -2 | 1 | **-0.5** | -1.41 | 6.13E-06 |
| 3846384 | STM14_4392 | | -1 | 0 | **-0.5** | 3.05 | 3.03E-07 |
| 571704 | STM14_0600 | | 0 | 0 | **0** | 4.1 | 1.63E-39 |
| 2060669 | STM14_2378 | | 0 | 0 | **0** | -1.52 | 0.0005 |
| 2746734 | STM14_3135 | *hmpA* | 0 | 0 | **0** | 1.79 | 7.28E-05 |
| 2746735 | STM14_3135 | *hmpA* | 0 | 0 | **0** | 1.79 | 7.27E-05 |
| 3243658 | STM14_3699 | *serA* | 0 | 0 | **0** | 1.48 | 5.09E-13 |
| 3402626 | STM14_3894 | | 0 | 0 | **0** | -1.23 | 7.87E-08 |
| 4185969 | STM14_4772 | | 0 | 0 | **0** | 3.17 | 4.96E-10 |
| 4185987 | STM14_4772 | | 0 | 0 | **0** | 3.17 | 4.96E-10 |
| 4185988 | STM14_4772 | | 0 | 0 | **0** | 3.17 | 4.96E-10 |
| 4415557 | STM14_5029 | *aceB* | 1 | 0 | **0.5** | 1.88 | 6.67E-06 |
| 1049501 | STM14_1130 | *ompF* | 1 | 1 | **1** | 1.08 | 4.46E-07 |
| 2060668 | STM14_2378 | | 2 | 0 | **1** | -1.52 | 0.0005 |
| 4185970 | STM14_4772 | | 2 | 0 | **1** | 3.17 | 4.96E-10 |
| 3758505 | STM14_4305 | | 1 | 3 | **2** | -1.41 | 6.13E-06 |
| 3846383 | STM14_4392 | | -1 | 6 | **2.5** | 3.05 | 3.04E-07 |
| 2060552 | STM14_2378 | | 5 | 1 | **3** | -1.52 | 0.0005 |
| 4802791 | STM14_5446 | *tsr* | 7 | 0 | **3.5** | -1.28 | 0.006 |
| 1049502 | STM14_1130 | *ompF* | 5 | 4 | **4.5** | 1.08 | 4.46E-07 |
| 3402625 | STM14_3894 | | 4 | 5 | **4.5** | -1.23 | 7.86E-08 |
| 2072703 | STM14_2394 | *fliJ* | 15 | -4 | **5.5** | -1.55 | 0.006 |
| 2072704 | STM14_2394 | *fliJ* | 19 | -6 | **6.5** | -1.55 | 0.006 |

*The *metJ* gene is excluded from these analyses due to artificial excision from the genome

1265 **Figure S1: Analysis of changes to the *S.* Typhimurium m$^6$A methylome in response to changing conditions reveals YhdJ as a dynamic methylase.** (A-C)
1266 Identification of motifs enriched in methylation sites unique to each of the comparisons in **Figure 2**. Motif enrichment was calculated by dividing the frequency of
1267 the motif among the uniquely methylated bases by the genome-wide frequency of that motif within that condition (*ex.* For Panel A, frequency of ATGCA*T within
1268 unique WT SPI-2 sites = 242 ATGCA*T sites/423 unique SPI-2 sites (0.57); frequency of ATGCA*T within all WT SPI-2 = 600 ATGCA*T sites/38,843 detected
1269 motifs (0.015); enrichment = 0.57/0.015 = 37.04). For all panels, only bases that could be confidently called methylated or unmethylated in all eight conditions in
1270 Methylation Experiment 1 were considered.
1271
1272 **Figure S2: A replication screen reveals methylation is highly reproducible across SMRT-seq experiments but highlights the value of performing biological**
1273 **replicates.** (A) Schematic for the Replication Methylation Experiment. Wild-type *S.* Typhimurium (Strain 14028s) or isogenic mutants were grown in LB media
1274 and DNA was harvested for SMRT-sequencing. (B) Approximately 97% of bases were called identically (methylated or unmethylated) in Methylation Experiment
1275 1 and the Replicate Methylation Experiments. (C) Only ATGCA*T and "other" sites (bases that do not map to one of the six motifs) change dramatically across
1276 tested conditions in the Replication Methylation Experiment. No ATGCA*T methylation was observed in Δ*yhdJ* mutants. (D) The observed Percent Methylation
1277 at each base is reproducible across experiments. The color of the hexagon represents the number of bases that fall at that point on the axes. $R^2$ values and trendlines
1278 represent the correlation across experiments. (E) Quantitative analysis reveals numerous sites are differentially methylated between wild-type and Δ*metJ*. Each dot
1279 represents the mean percent methylation in wild-type bacteria across the two experiments subtracted by the mean methylation in Δ*metJ* bacteria for each adenosine
1280 confidently called in both experiments. Blue and green dots mark bases where the mean difference is ≥10%. (F) Quantification of unique methylation sites in the
1281 Replication Experiment. For Panels C-F, bases were only included in the analysis if the base could confidently be called methylated or unmethylated across
1282 conditions. (G) Venn diagram is based on binary measures of differential methylation in the combined dataset. Sites identified by the binary analysis were examined
1283 in our quantitative dataset in order to identify changes in the percent methylation. In the graphs "Total" refers to all differentially methylated sites under that
1284 condition, and differentially methylated sites are then broken down by motif. For motifs where no differentially methylated sites were present, a single dot is listed
1285 at 0%. For shared sites, the absolute value of the difference between bases are shown and thus the numbers are agnostic to whether methylation is higher in either
1286 condition. Bars mark the median.
1287
1288 **Figure S3: ACCWGG is enriched in "other" differentially methylated sites.** (A,B) The 40 base pairs flanking sites that were differentially methylated between
1289 wild-type and Δ*metJ* bacteria grown in LB in our Combined Dataset (A) or between wild-type bacteria grown in LB and SPI-2 inducing conditions in Methylation
1290 Experiment 1 (B) but did not map to one of our 6 motifs were plugged into the MEME software (95) in order to identify overrepresented motifs. ACCWGG, a
1291 common miscall for the m$^5$C motif CCWGG, was identified in both comparisons.
1292
1293 **Figure S4: Conditions in the RNA-seq experiments cluster with previously published datasets.** PCA analysis comparing data from the Δ*metJ* RNA-seq
1294 experiment (Supplemental File 4; "Exp 1") and the Δ*yhdJ* experiment (Supplemental File 5; "Exp 2") cluster with data from Kröger *et al*. (96). The LB condition
1295 used from Kröger *et al*. was early stationary phase, for which the OD600 (~2.0) most closely matches the OD600 used in this study (1.5-2.0). Both the SPI-2
1296 inducing condition and the SPI-2+MgCl2 condition were included from Kröger *et al*. Medias separate along PC1, which accounts for 53.5% of the variation. Each
1297 condition from this paper is completed in triplicate (with three dots represented on the plot), each Kröger condition in duplicate (two dots on the plot).
1298
1299 **Figure S5: *flhDC* expression is reduced in Δ*metJ*.** (A) In contrast to our previous findings (91), *flhD* expression is reduced in Δ*metJ* bacteria by qPCR. Bacteria
1300 in late log phase growth in LB were harvested, RNA was stabilized, and RNA was extracted and quantified as described in the methods. Fold change (Δ*metJ*/wild-
1301 type) is expressed as $2^{-\Delta\Delta CT}$, where *flhD* transcript was normalized to the *rrs* gene. Each dot represents the average of 2-3 technical replicates. (B) Endogenous
1302 tagging of *flhC* confirms reduced *flhDC* expression in Δ*metJ* bacteria. A C-terminal 3xFLAG tag was added to the *flhC* gene, and abundance of the protein was
1303 measured by western blotting. Specificity of the FLAG antibody to FlhC-3xFLAG was confirmed by comparing to a wild-type, untagged *S.* Typhimurium strain.
1304 FlhC-3xFLAG abundance was quantified following correcting for loading by normalizing to total protein, and data are presented relative to wild-type (WT) *flhC*-

1305 *3xFLAG S.* Typhimurium. Each dot represents an independent experiment, bars represent the mean, and error bars the standard error of the mean. For A and B, p-
1306 values are from a one sample t-test performed on the log transformed data comparing the log(values) to 0.
1307
1308 **Figure S6: Stratification of binary data does not reveal correlation between differentially expressed genes and differentially methylated genes.** (A-C)
1309 Fisher's Exact Test does not reveal an association between differential expression and methylation when the statistical cutoff for differential expression is changed
1310 to $\log_2$FC>1.5 and FDR corrected p-value<0.05 for any condition. For wild-type LB vs SPI-2 comparisons, there are also no statistical associations when (D) the
1311 statistical cutoff for differential expression is changed to $\log_2$FC>2.0, or when the data are stratified by (E) direction of gene expression change in LB, (F) direction
1312 of gene expression change in SPI-2 media, (G) differentially methylated bases upstream of genes, (H) differentially ATGCA*T methylation, (I) differential GA*TC
1313 methylation. Uniquely methylated genes are plotted in the condition under which they are methylated (*e.g.* for panel B, a gene that has a methylated upstream base
1314 in LB but not SPI-2 media would be plotted as part of "LB"), but are agnostic to the direction of effect for the expression change except in Panels E and F. Data
1315 for Panel B from the combined dataset, all other data from Methylation Experiment 1.
1316
1317 **Figure S7: Stratification of quantitative data does not reveal additional correlations between differentially expressed genes and differentially methylated**
1318 **genes.** (A-C) Fisher's Exact Test does not reveal an association between differential expression and methylation when the statistical cutoff for differential expression
1319 is changed to $\log_2$FC>1.5 and FDR corrected p-value <0.05 for any condition, except for wild-type bacteria with increased methylation relative to Δ*metJ* bacteria
1320 in SPI-2 media where an association was also seen with the less stringent cutoff. (D-F) Fisher's Exact Test does not reveal an association between differential
1321 expression and methylation differentially methylated bases when only differential methylation upstream of genes is considered. (G-I) Fisher's Exact Test does not
1322 reveal an association between differential expression and methylation when the definition of "Differential Methylation" is shifted to sites where (1) the base is
1323 ≥99% methylated in one condition, and (2) has a difference of ≥10% between the two conditions, except for wild-type bacteria with increased methylation relative
1324 to Δ*metJ* bacteria in SPI-2 media where an association was also seen with the less stringent cutoff. Differentially methylated genes are plotted in the condition
1325 under which they are hypermethylated (*e.g.* for panel D, a gene that has an upstream base with increased methylation in LB but not SPI-2 media would be plotted
1326 as part of "LB"), but are agnostic to the direction of effect for the expression change. Data for panels B, E, and H from the combined dataset, all other data from
1327 Methylation Experiment 1.
1328
1329 **Figure S8: Differentially methylated sites from Sánchez-Romero *et al* (98) do not correlate with reproducible changes in gene expression.** (A,B) *carA* (A)
1330 and *dgoR* (B) do not show reproducible changes in gene expression between LB grown and SPI-2 induced bacteria. (C,D) Other genes have reproducible effects
1331 in the dataset including (C) *prgH* and (D) *ssaT.* Exp 1 refers to the Δ*metJ* RNA-seq experiment (Supplemental File 4) and Exp 2 refers to the Δ*yhdJ* RNA-seq
1332 experiment (Supplemental File 5). P-value calculated from FDR.
1333
1334 **Figure S9: Methylation upstream of *flhDC* does not contribute to the Δ*metJ* motility defect.** The -278 GATC sequence is not required for the impacts of Δ*metJ*
1335 on motility. Motility on soft agar was measured six hours after inoculating the agar and following migration at 37°C, each dot represents the average of 3-5 technical
1336 replicates, data were normalized to the grand mean prior to plotting or performing statistics, and p-values were generated by two-way ANOVA with Sidak's
1337 multiple comparisons test.
1338
1339 **Table S1: Bacterial strains used in this study**
1340
1341 **Table S2: Plasmids used in this study**
1342
1343 **Table S3: Oligonucleotides used in this study**

1344
1345 **Table S4: Percent methylation compared to previous hypomethylation studies**